

Review

The Influence of Web Holes on the Behaviour of Cold-Formed Steel Members: A Review

Vladimir Živaljević , Đorđe Jovanović, Dušan Kovačević and Igor Džolev * 

Faculty of Technical Sciences, University of Novi Sad, Trg Dositeja Obradovića 6, 21000 Novi Sad, Serbia; zivaljevic.vladimir@uns.ac.rs (V.Ž.); djordje.jovanovic@uns.ac.rs (Đ.J.); dusan@uns.ac.rs (D.K.)

* Correspondence: idzolev@uns.ac.rs

Abstract: The use of cold-formed steel (CFS) members in structural engineering has been on the increase recently due to a wide range of benefits. The placement of electrical and/or plumbing installations within the floor or wall thickness requires that members are being manufactured with holes along the web, inevitably affecting their resistance. This article aims at providing a useful and comprehensive overview of the existing literature regarding CFS members with web holes. Experimental and numerical research on CFS members with web holes subjected to pure compression, bending, web crippling and shear is outlined and discussed. Although research on these types of members date back to the early 1970s, the greatest progress in the research field of CFS members with web holes was achieved during the past 15 years; hence, mostly the research conducted during this period was addressed. Additionally, design proposals are summarised for each of the aforementioned stress states. A brief description of the main concepts of design presented in four principal design codes, as well as numerical solution methods for predicting global, local, and distortional buckling modes, is also presented, aiming to collect the accessible up-to-date knowledge of CFS members with holes and identify areas that were modestly covered by previous research.

Keywords: cold-formed steel; web holes; experimental investigations; numerical analyses; buckling; ultimate strength; review



Citation: Živaljević, V.; Jovanović, Đ.; Kovačević, D.; Džolev, I. The Influence of Web Holes on the Behaviour of Cold-Formed Steel Members: A Review. *Buildings* **2022**, *12*, 1091. <https://doi.org/10.3390/buildings12081091>

Academic Editors: Keerthan Poologanathan, Gatheeshgar Perampalam, Shanmuganathan Gunalan and Marco Corradi

Received: 5 June 2022
Accepted: 19 July 2022
Published: 26 July 2022

Publisher's Note: MDPI stays neutral with regard to jurisdictional claims in published maps and institutional affiliations.



Copyright: © 2022 by the authors. Licensee MDPI, Basel, Switzerland. This article is an open access article distributed under the terms and conditions of the Creative Commons Attribution (CC BY) license (<https://creativecommons.org/licenses/by/4.0/>).

1. Introduction

Cold-formed steel (CFS) members with web holes have been used widely in the recent past due to their lightweight structure, cost-effective advantages over the entire construction cycle, structural efficiency, practicality, etc. They are often employed as columns [1–16], beams [3,4,17–31], and the load-bearing structures of sheathed panel shear walls, light frame strap-braced walls, partition walls, curtain/facade walls, floor joists, etc. Mainly, the C-, Z-, and Σ -sections and their varieties are used. The most common cross-section shapes and 3D models of CFS members with circular web holes are presented in Figure 1. These elements are often produced with holes along the web to facilitate electrical, heating or plumbing installations. Consequently, a resistance decrease of the member is expected. This issue has been addressed by adding stiffeners along the section [9,16,32] and hole edges [4,13–15,22,28,33–36]. Since the behaviour of CFS elements is dictated by instability effects rather than the yield of the material, the size and location of web holes along the element can prove to be an important factor [6,8,14,17,18,21,23–25,28,30,37–46].

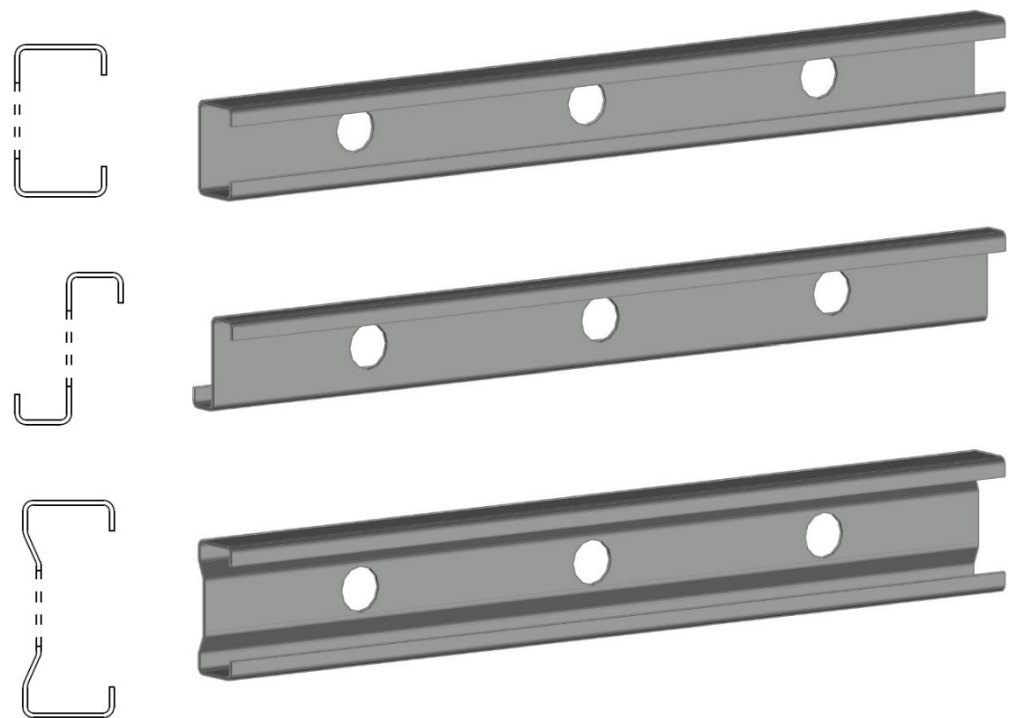


Figure 1. Most common cross-section shapes of CFS members: C-section, Z-section, and Σ -section.

Previous research was mainly focused on short- and medium-length elements, since they are prone to distortional and local buckling. In such cases, the location of a hole may coincide with the position where the maximum displacement of the buckling half-waves is expected [2]. Longer elements tend to buckle in a global mode, assuming that the ultimate member resistance is not influenced by the position and the number of web holes along the element. Although the majority of research has been focused on elements subjected to pure compression or bending, in recent years, web crippling [33–36,47–65] and shear [43–46,66–73] behaviour have been analysed as well. However, a commonly occurring case in the engineering practice of combined compression and bending [32] should have attracted more attention from researchers. This issue has been addressed when it comes to CFS members without web holes [74–84] and CFS members with small and densely arranged perforations typical for rack uprights [85–88].

The aim of this work is:

- To provide an overview of the existing research and knowledge on CFS members with web holes subjected to compression, bending, web crippling and shear;
- To summarise the chronological development and up-to-date design recommendations in one place;
- To point out the courses of future work and cases which might be examined in more detail.

Since the structural design, unlike other technical branches worldwide, is regulated by law, i.e., by the prescribed set of technical rules that must be followed during the design and construction of any facility, design codes in the field of CFS elements will be presented firstly. Undoubtedly, design codes develop over time, based on the results of scientific research. Mainly, North American (S100-2016) [89], European (EN 1993-1-3) [90], Australian/New Zealand (AS/NZS 4600) [91], and Chinese (GB 50018) [92] standards are addressed. The main concepts of design are also briefly described: (i) the Effective Width Method (EWM) and (ii) the Direct Strength Method (DSM). Since the most recent editions of the CFS design codes are focusing on the DSM as the main design concept, numerical solutions that accompany the design process are described as well. In the subsequent chapters, the research on the behaviour due to pure compression, bending, web crippling

and shear states is outlined. Regardless of CFS structures being thin-walled and, therefore, sensitive to fire, research related to CFS members with web holes subjected to thermal loads is not discussed in this paper.

2. Method

Articles for this review were, for the most part, acquired from the Science Direct, Google Scholar, and ASCE Library databases. The research methodology employed in this study consisted of keyword and phrase searches and categorisation. The used search terms were “Cold-formed steel”, “Web holes”, “Experimental testing”, “Numerical Analyses”, “Cold-formed steel design”, and “Distortional and local buckling”, resulting in 4817 Science Direct, 1680 Google Scholar, and 390 ASCE Library papers. Further reliability criteria included only peer-reviewed research publications and reported experimental tests conducted entirely in specialised laboratories, under controlled environmental and physical conditions, thus enabling reproducibility and reducing potential threats to validity.

The applied inclusion criteria were the following:

- Papers published as journal articles and conference papers;
- Papers published in the field of civil and structural engineering;
- Papers accessible in full-text.

Further, exclusion criteria were:

- Duplicates;
- Papers not written in English;
- Papers published before 2010;
- Papers in which members were subjected to thermal load.

After a detailed reading and classification of selected papers, the authors realised that the review would seem incomplete without the presentation of the chronological development and agreed that papers of an earlier date than 2010 should also be included. The exclusion criteria were then re-established.

The classification of papers was established on several levels. The first one was based on the type of stress state applied on the examined members, i.e., compression, bending, web crippling, and shear. The main sections of this review are titled accordingly. The second stage of classification considered the type of the cross section. In most of the studies, C-sections with un-stiffened web holes were the subjects of examination, while, in the past decade, C-section members with edge-stiffened holes have attracted major interest. Several studies were conducted on sections other than C-shaped. Finally, the last stage of the classification indicated the publishing date. In each subsection, papers were reviewed as per the chronological timeline, aiming to give a clear perception on the development of research methodology, experimental procedures, and design equations.

3. Design Codes and Theory

3.1. Design Codes

The first code for the design of CFS members was published in 1946 by the American Iron and Steel Institute (AISI) [93]. Over the years, codes have evolved, covering two completely different design methods for CFS members: (i) The Effective Width Method (EWM) and (ii) the Direct Strength Method (DSM). AISI S100-2016 and AS/NZS 4600 incorporate both the DSM and EWM and provide instructions for the design of CFS elements with web holes. The EN 1993-1-3 and GB 50018 design codes, however, are based only on the EWM and do not provide specific instructions for elements with web holes. Moreover, the influence of both the number and the arrangement of holes along the element is not considered in the calculation of member resistance in any of the above-mentioned design codes. EN 15512 [94] provides guidelines for the design of elements with small and closely-spaced perforations along the element, such as in the case of steel rack elements. Accordingly, elements subjected to compression should be designed by testing, while the use of a design procedure is allowed for the elements subjected to tension.

The EWM handles usual types of CFS cross-sections and requires a complex, iterative procedure [95], which makes the automation of the design procedure necessary. The design strength calculation in [90] includes axial tension and compression, bending, shear, torsion, and their interactions, while inelastic reserves in CFS sections are omitted. Since the presence of holes is introduced via the net cross-sectional properties, the most unfavourable arrangement of holes must be taken into account.

The calculation of member resistance according to the DSM is based on member elastic buckling solutions that utilise gross cross-section properties, and unlike the EWM, the DSM considers inelastic reserve strength. The influence of holes is taken into account through the weighted average cross-sectional properties. According to AISI S100-2016, for elements subjected to pure tension, the member strength is determined based on the yield stress and the net cross-section. In cases of pure compression or bending, member resistance is calculated for three limit states: (i) yield and global buckling, (ii) local buckling interacting with yielding and global buckling, and (iii) distortional buckling. The shear strength and web crippling strength calculation in AISI S100-2016 are defined only for C-section elements. The provisions defined in this case are only valid under certain limitations, by which the nominal shear strength and the nominal web crippling strength of the C-section web without holes are reduced by the appropriate factor.

3.2. Numerical Solutions

Several numerical solution methods for predicting global, local, and distortional buckling modes and the corresponding critical load values of members without holes are in use: the shell finite element method (sFEM), the finite strip method (FSM), and generalized beam theory (GBT). The FSM and GBT methods are capable of completing this task for the selected isolated (“pure”) or arbitrarily combined (“coupled”) modes [96].

AISI S100-2016 allows the use of sFEM, FSM, and GBT for the determination of the buckling modes. However, only the sFEM is able to capture the effects of the web holes. Moen and Schafer [3] studied the differences between the FSM and sFEM eigenbuckling analyses. The predicted critical load with the sFEM was lower than the one computed from the FSM, since the latter was unable to capture the effects of web holes. For that reason, a simplified FSM for computing the global, distortional, and local critical load of columns and beams was proposed. Moreover, a simplified FSM for these cases is currently also being developed by Grey and Moen [4], Casafont et al. [97], and Smith and Moen [7]. On the other hand, EN 1993-1-3 provides provisions only for the numerical methods to be used for the examination of the effects of the distortional buckling load.

While the conventional FSM solutions for simply supported (S-S) members calculate the first buckling load for a wide range of member lengths, constrained FSM (cFSM) solutions for general boundary conditions are orientated towards the investigation of higher modes for a specified physical length. In that manner, the cFSM solutions for general boundary conditions closely resemble the FEM ones [98]. cFSM is introduced in the open-source software CUFSM (Ver. 5.04) [96,99]. The inclusion of holes in a buckling analysis in CUFSM is currently under development. However, Moen and Schafer [27] suggest creating a model with a zero-thickness strip element across the hole in order to capture its effect.

The propositions for the design of CFS members with holes in the current edition of AISI S100-2016 are based on the comprehensive research presented by Moen [100]. In this research, CFS beams and columns with holes are analysed using the sFEM and FSM analyses. A total number of 24 column specimens were experimentally tested, whereas simulated experiments on 125 laterally braced beams were conducted using the ABAQUS software [101]. A new set of design equations for the ultimate strength was developed in order to properly include the effects of holes. A summary of the experimental and numerical research for columns was published in [5]. The theoretical background of the DSM approach and the design examples for CFS beams with holes were given in [27].

Research on the stability behaviour of C-section columns with web holes with simple and complex edge stiffeners and the comparison of the numerical and DSM results was

conducted by Wang et al. [10]. They demonstrated that the existence of holes can affect the member resistance, although neither shape nor spacing has a crucial impact. Although the current DSM design equations lead to slightly different strength values compared to the FEM analyses, it was concluded that the DSM is still applicable in cases of perforated columns with simple and complex edge stiffeners.

Similarly to the cFSM, GBT also shares the modal nature of the analysis of the elastic buckling behaviour of thin-walled members. As a generalization of classical beam theory, GBT incorporates cross-section in- and out-of-plane deformations by introducing additional degrees of freedom. The recent progress in the field of GBT has been made through the development of the open-source software GBTUL (Ver. 2.06) [102–106]. However, the inclusion of holes in the buckling analysis in GBTUL is currently not provided.

Unlike the FSM and GBT, the advantages of the sFEM are recognised in the definition of arbitrary geometry (Moen and Schafer [2], Kulatunga and Macdonald [6], Wang et al. [9]), resulting in the sFEM being the most precise method for determining the elastic, as well as plastic, buckling mode shapes.

4. Pure Compression

4.1. C-Section Stub Columns

One of the the first experimental investigations of CFS elements with holes was conducted by Yu and Davis [1,59]. The reduction of the buckling load and post-buckling strength of a stub column composed of two C-sections with circular and square holes was evident. However, the post-buckling strength of the elements was not influenced by the shape of the hole.

C-section stub columns with punched web holes were experimentally tested by Loov [37] with the intention to propose equations for the effective width of the unstiffened web portion alongside the holes. A total number of 36 specimens with one square and two circular web holes were tested. The size of the holes was kept constant, while the web depth (i.e., the web effective area) was varied. As such, the stub columns could not be appropriately designed by the employment of the CSA S136-1974 [107] design equations.

The influence of holes on member effective area was further investigated by Sivakumar in [108,109] on 42 specimens with one circular, square, or elongated hole at the mid-length and 6 specimens without a hole. The length of specimens was chosen in order to induce the local buckling shape. Comparison between the experimental and design ultimate load (EWM in the former version of the US code [110] and in CSA S136-1974) showed that both design procedures overestimated the strength of the sections; hence, a revision was necessary. Once more, the shape of an opening appeared to be an insignificant parameter.

The influence of the size and position of rectangular holes in the cross-section on the ultimate compressive strength was experimentally investigated on 63 stub columns by Pu et al. [38]. Three different hole arrangements were examined: (i) at a quarter of the web depth away from the edge in the same side, (ii) at the centre of the web, and (iii) at web edges. The resistance decrease was most pronounced in the cases where the holes were located in the effective area, i.e., at the edges of the web.

Most of the research, on the other hand, was performed numerically. In order to provide the effective design width equations for the determination of the ultimate strength, Abdel-Rahman and Sivakumar [39] conducted a numerical investigation on CFS C-section stub columns with various hole sizes. The accuracy of the proposed equations was validated through a comparison with the results of several experimental studies from the existing literature. Due to biaxial symmetry, only one quarter of the stub column was modelled using sFEM. Uniformly distributed compressive displacement was imposed via a rigid plate element. The interface with the loaded edge of the stub column was modelled using short rigid truss elements. Moreover, a double sine-wave initial geometric imperfection was introduced. Experimental observations in Abdel-Rahman's Ph.D. dissertation [111]

showed that non-symmetric buckling modes do not govern the buckling problem; hence, symmetry boundary conditions could be applied.

A simplified design formula for the ultimate load capacity of CFS C-section stub columns with holes was developed by Shanmugam and Dhanalakshmi [40]. A numerical parametric study was conducted, varying plate slenderness, opening size, and ultimate-to-squash load ratio. The length of specimens was chosen to induce local buckling. Moreover, linearly distributed residual stresses through the plate thickness and an initial geometric imperfection in the form of several superimposed buckling modes were included in the FEM model. The FEM model and the proposed design equation were validated based on experimental and numerical results in the existing literature.

4.2. C-Section Intermediate-Length Columns

Since the majority of the experimental tests were conducted on stub column specimens, Moen and Schafer [2] conducted research on both short- and intermediate-length specimens. Two C-section types with different web depths were studied in order to examine the correlation between the elastic local and distortional buckling and the response of the CFS columns with holes. The position of the holes was determined to coincide with the location of the maximum displacement of the distortional buckling half-waves (one web hole for short- and two for intermediate-length columns). A minor resistance decrease was noticed due to the presence of slotted holes. However, the post-peak response and ductility were noticeably influenced not only by the presence of web holes, but also by the length of the member and the cross-section type.

Although considered appropriate for everyday engineering use, shell FE models are usually demanding to develop. The accuracy and efficiency of the numerical model are considerably affected by the selection of the proper FE type and mesh density and the appropriate boundary conditions. Additionally, a subjective visual identification of buckling modes is also necessary. In order to improve design efficiency, Moen and Schafer [3] presented simplified methods for approximation of the global, distortional, and local critical elastic buckling loads of CFS columns with holes.

Research on load transfer, stress distribution, and local buckling failure modes of simply supported perforated plates and C-sections was carried out by Yao and Rasmussen [41]. For this purpose, the isoparametric spline finite strip method (ISFSM) [112,113] was used. The emphasis was put on the von Mises membrane stress distributions at various loading rates and for different material stress–strain curves, considering several different hole sizes and arrangements. The member behaviour and strength were mostly affected by the hole width change, whereas the influence of hole length and spacing was less pronounced.

The effects of the web hole position on the ultimate strength of C-sections were experimentally and numerically investigated by Kulatunga and Macdonald [6]. Tests revealed that the failure was influenced mostly by local buckling, while the greatest resistance reduction occurred in cases where holes were located in the proximity of the member ends.

Additional experimental and numerical research was carried out by Kulatunga et al. [8] in order to examine the influence of the shape of the holes on the buckling behaviour of CFS C-sections of intermediate length. Tests conducted on 10 specimens with one circular or elongated hole showed the shape of the hole to be negligible in considering the reduction of the member strength. However, for the 10 specimens with two web holes, the strength reduction was higher for members with circular web holes than for those with elongated ones with the same area. It was noticed that local and distortional buckling occur at load levels of about 50% and 70% of ultimate strength, respectively. The acquired results were also compared with the predicted ultimate loads obtained by AISI S100-2012 [114], BS 5950-5 [115], and EN 1993-1-3. All of the considered design codes were proved to be conservative.

The behaviour of CFS columns with holes was examined in detail in a comprehensive research study by Yao and Rasmussen [42], and the results were summarised in a two-part research paper [11,12]. A numerical parametric study was presented for columns of

various cross-section types (C, stiffened C, Z, rack, and hat sections), subjected to local, distortional, and global buckling. Corner restraints were applied at certain cross-sections in order to induce a particular failure mode (local or distortional). A wide range of hole dimensions and spacing, material properties, and initial geometric imperfections were taken into account.

In the second part of the research, two sets of design equations for thin-walled columns with web holes were proposed. The proposed methods were compared with the existing DSM equations in AS/NZS 4600 and Design Option 4 presented by Moen and Schafer [5]. It was concluded that the greatest variations in the predictions resulted from the interaction of buckling modes rather than the presence of holes. The level of hole influence on the member resistance was dependant on the failure mode, cross-section type, and dimensions.

4.3. C-Section Columns with Edge-Stiffened Web Holes

Over the past few years, new family of C-sections with edge-stiffened web holes have been developed to overcome the limitations of traditional CFS C-sections with web holes. Design rules for CFS channels with edge-stiffened holes are not yet available in AISI S100-2016 and AS/NZS 4600. A C-section CFS member with edge-stiffened holes is depicted in Figure 2.

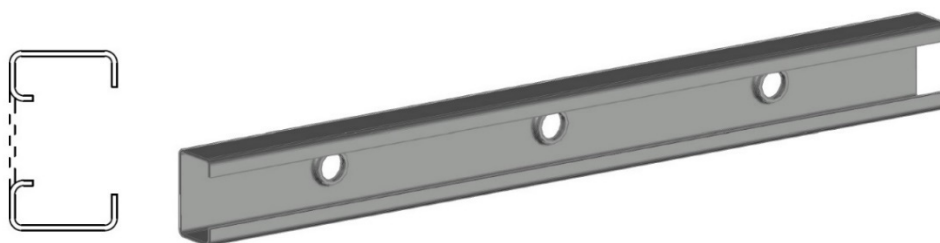


Figure 2. CFS member with edge-stiffened holes.

Members with unstiffened and edge-stiffened holes and members without holes were experimentally compared by Chen et al. [13]. Test results were validated with FEM analyses, followed by a detailed parametric study [14] aiming to determine the influence of hole spacing and member length on compression resistance. Compared to members without holes, resistance was higher in cases with edge-stiffened web holes by as much as 21% for the case of members with seven openings. However, the same members but without stiffeners along the holes exhibited a 20% reduction in the resistance. Moreover, local deformation, previously occurring in close proximity to the hole, shifted to the area between two adjacent holes.

The study further included variables such as column slenderness, stiffener length, fillet radius, hole size, location, and spacing. Results obtained numerically yielded much greater member resistance than that calculated by AISI S100-2016 for CFS channels with unstiffened holes, which underestimated the influence of stiffeners. Hence, improved design equations for different ranges of column slenderness were proposed, in which the axial capacity predicted from the equations of Moen and Schafer [2,3,5,116] was factorised with coefficients depending on stiffener length, hole spacing, and stiffener fillet.

The same group of authors put to experimental and numerical testing [15] commonly used back-to-back built-up channels. A total of 27 specimens were tested, in which the influence of edge-stiffened holes was investigated for 9 of them. Additionally, 18 test were conducted on single channels in order to study the effect of composite action. Specimens of three different lengths, aiming to take into account the influences of different slenderness and one web hole at a mid-length of a member, were examined. Measurement of the initial geometric imperfections and tensile tests of the coupons from flat and corner zones of a cross-section were carried out before compression tests. Members with edge-stiffened holes demonstrated higher axial capacity by 6.6%, while the capacity of the same section with un-stiffened holes was reduced by 12.4%, both compared to that of a plain channel.

Finally, comparison between the established axial capacities of specimens with holes and the design equations provided by Moen and Schafer [2,3,5] for single channels revealed the conservativeness of those equations.

The problem of predicting buckling behaviour of CFS columns and beams with edge-stiffened holes was addressed by Grey and Moen [4]. The buckling behaviour was examined on C-sections with stiffened holes by means of the FSM, while an sFEM eigenbuckling analysis was used to verify the results of the simplified method. The local buckling was reduced to a minimum in the vicinity of the hole, while buckling half-waves were formed between the holes. For the determination of the global buckling load, the “weighted average” cross-section properties were employed, which accurately predicted the critical loads for flexural and torsional buckling. Since the removal of the material at the position of the hole reduces the bending stiffness and the edge stiffeners around the hole increase it, a new equation for effective web thickness was derived.

4.4. Other Sections

In order to increase the cross-sectional stiffness, a C-section may be manufactured with an additional inward return lip, also called a G-section. The behaviour and ultimate compression load of such members with holes were experimentally and numerically investigated by Wang et al. [9]. Besides the G-section, a Σ -section (with complex edge stiffeners and Σ -type web stiffeners) stub and intermediate columns with holes were also studied. The Σ -section members with holes demonstrated an increase of about 30% to 50% in ultimate strength in comparison to the perforated G-section members. However, the resistance decrease of the C-section due to the presence of holes was about 6%, whereas the resistance of the perforated Σ -section elements decreased by about 25%. While the local buckling mode was the leading failure mode in cases of stub C-sections, the combination of the local and distortional ones was predominant in cases of stub Σ -sections. The failure mode of medium-length columns was manifested as a combination of the local and flexural (C-section) and local, distortional, and flexural (Σ -section). Moreover, a comparison of DSM and FEM analysis results revealed that the current design equations for C-sections with holes adopted in AISI S100-2016 can also be applied for the perforated channels with complex edge stiffeners.

The behaviour of compressed G-section members with holes was experimentally and numerically investigated by Xiang et al. [16], on 20 specimens without holes and 16 specimens with holes. Besides the usual web holes, a great number of smaller perforations were added in the vicinity of the larger openings. Due to the presence of holes, not only a resistance reduction but also a change in the deformed shape was noted. Local shapes and interaction between local and flexural shapes due to failure were documented. In addition, the deformation shape of the column also varied for different hole locations. The reduction in member strength was proportional to the increase in the hole dimensions, while the deformed shape in most cases remained unchanged.

Stub, medium-long, and long columns of built-up I-sections with holes and complex edge and web stiffeners were experimentally tested by Wang et al. [32]. In cases of stub and intermediate columns, the governing failure mode was the distortional, since the web stiffeners prevented the occurrence of local web buckling, as well as decreasing the deformation in the proximity of the hole. Contrarily, the global flexural mode governed the failure of long columns, indicating that web stiffeners had an insignificant influence on their resistance. A parametric study on Σ -shaped built-up I-section members with holes was carried out as well, varying member length, cross-section dimensions, and hole size, to investigate the optimal hole-depth-to-web-stiffener-height ratio (d/h_s). It was found that the optimal d/h_s was in the range of 0.7–0.8. Since the DSM equations for built-up sections were still not developed, design equations by Moen and Schafer [5] and Yao and Rasmussen [12] were applied for the purposes of calculation checks. It was observed that these methods predicted the buckling capacity of the studied members fairly accurately.

4.5. Comparisons and Discussion

Until the beginning of the 21st century, the axial capacity of CFS members was determined using methods that employed only the cross-sectional parameters, neglecting a very important factor regarding the behaviour of CFS members—the tendency to buckle in forms other than global (flexural). With the development and expansion of the DSM method, the importance of the dominant buckling shape became evident.

Appendix A Table A1 provides summarised design equations for elements in pure compression by various authors. Shanmugam and Dhanalakshmi [40] proposed the procedure that relies on the web flat height-to-thickness ratio, as well as cross-sectional properties. Since their research was based on stub columns, the possible diversity of the buckling modes was neglected. Among the first to do so, in the early 2010s, Moen and Schafer [5] proposed a set of DSM equations for compressed members with web holes that, by extension, took into account the possibility of not only flexural but also local and distortional buckling. Several years later, Yao and Rasmussen [12] slightly revised Moen’s and Schafer’s procedures for local and distortional buckling. Parallel to Moen’s and Schafer’s work, Grey and Moen [4] proposed equations for columns with edge-stiffened holes. Nearly a decade later, Chen et al. [14] came to the conclusion that the equations from [5] could also be used for members with edge-stiffened holes, if properly modified.

Prediction curves for elements sensitive to global buckling according to AISI S100-2016 for the elements without holes and according to Moen and Schafer [5] (DSM option 6) for elements with holes are depicted in Figure 3. Prediction curves are presented for the axial yield strength of net cross-section-to-axial yield-strength-of-gross cross-section ratios (P_{yn}/P_y) equal to 0.8 and 0.9. Additionally, experimental data for the same ratios obtained in Moen’s Ph.D. dissertation [100] are given. Since, for a slenderness (λ_c) of less than 1.5, the procedure for determining the compressive strength of elements without holes given in AISI S100-2016 yields results that overestimate the compressive strength, the corrections introduced in [5] took this effect into account. It can also be observed that, for a slenderness of 1.3 and above, the influence of web holes on member strength is negligible.

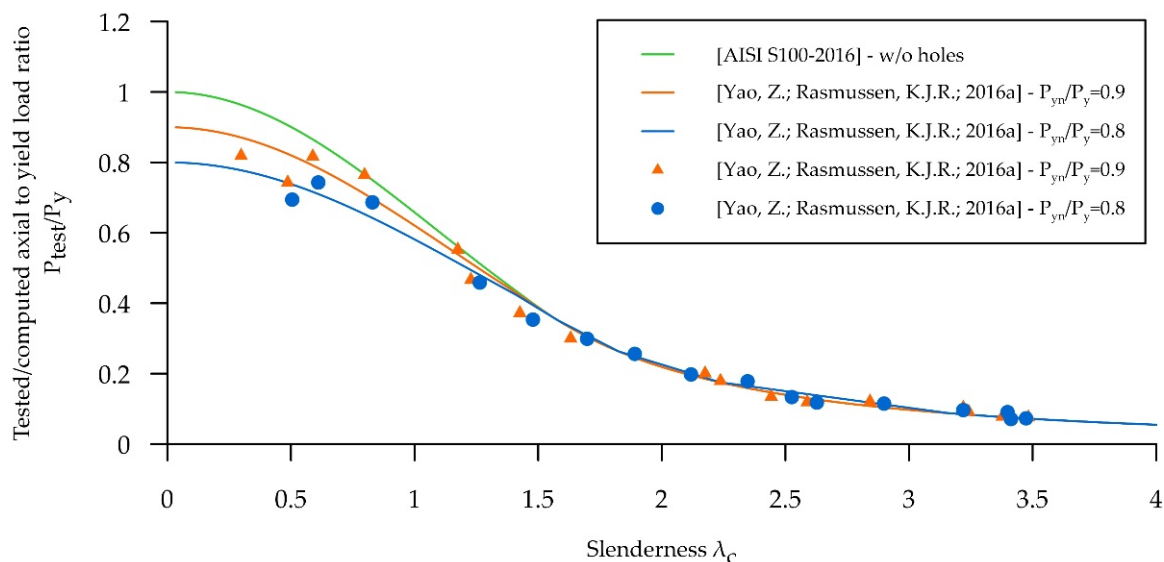


Figure 3. DSM prediction curves and experimental data for CFS columns predisposed to global buckling [11,89].

For the elements prone to distortional buckling, the DSM prediction curves according to [5,12,89] and the results of the experimental research carried out by Moen [100] and Moen and Schafer [2] are depicted in Figure 4. In [2], both stub and intermediate columns were tested. Stub columns exhibited buckling failure as the combination of the local buckling in the vicinity of the applied load and the distortional buckling along the column length.

Both one- and two-half-wave distortional buckling forms appeared, indicating that the geometric imperfections should not be neglected. The group of intermediate columns exhibited distortional deformation as the load approached the value of $0.70P_{test}$, while the instantaneous global flexural–torsional buckling appeared after the peak load. The prediction curve according to AISI S100-2016 applies to the elements without holes, while for the elements with holes, it is identical to the curve proposed by Moen and Schafer [5] (DSM option 4). Prediction curves according to [98,113] are given for the P_{yn}/P_y ratios of 0.6 and 0.8. In cases of high slenderness (λ_d), the resistance is controlled by the elastic buckling; hence, the results are not on the safe side. For lower slenderness, yielding and inelastic buckling have a greater influence; therefore, the proposed equations yielded slightly higher values of compressive strength than those obtained experimentally.

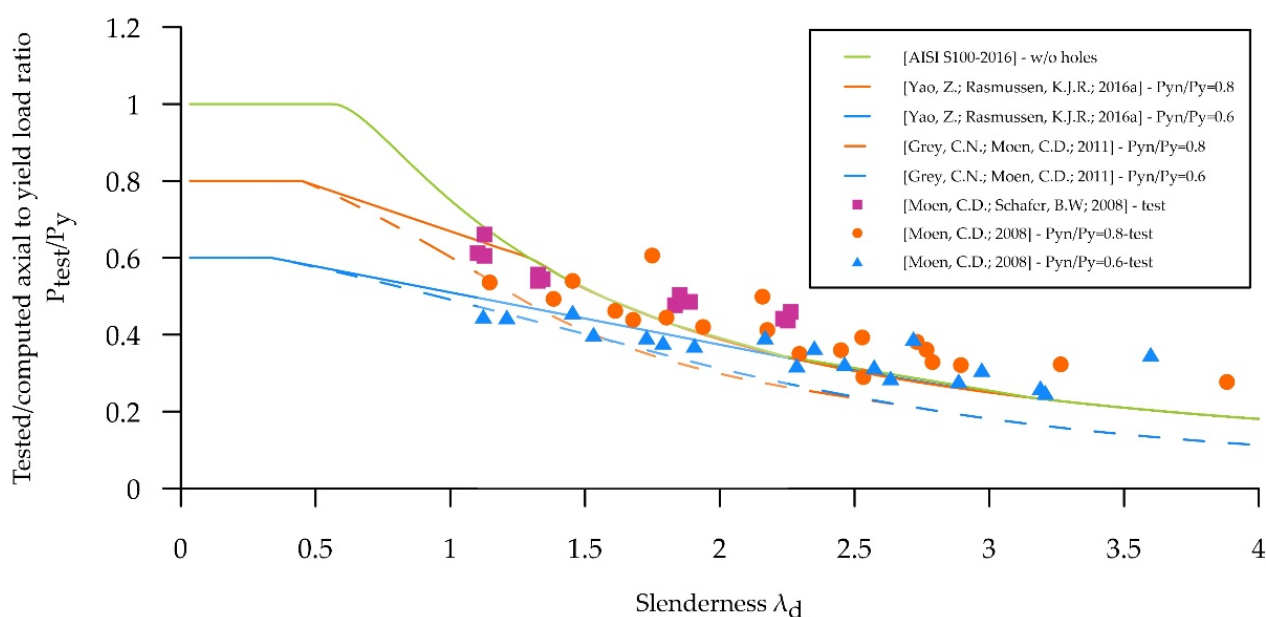


Figure 4. DSM prediction curves and experimental data for CFS columns predisposed to distortional buckling [2,4,11,89,100].

The DSM prediction curve for the elements predisposed to local buckling according to [5] and the results of the experimental research carried out by Moen and Schafer [2] and Kulatunga and Macdonald [6] are shown in Figure 5. In addition to the distortional half-wave along the length of short columns in [2], the concentration of plastic deformation occurred in the flanges as well as in the web on one or the other side of the hole, initiating local deformation. Concerning the intermediate-length columns, a number of specimens manifested local deformation of the web between the holes, which was suddenly changed to a distortional shape near the peak load. This change in the dominant deformation shape was followed by a slight drop in load. In [6], local deformation of the cross-section was developed in the proximity of the hole. However, a more descriptive presentation of experimental results is needed in order to draw a conclusion on the behaviour of the tested specimens. The prediction curve in AISI S100-2016 matches the one proposed by Moen and Schafer [5], which is provided for a P_{yn}/P_y ratio of 0.8. Experiments revealed that the compressive strength of the elements was slightly higher than the one computed from [5].

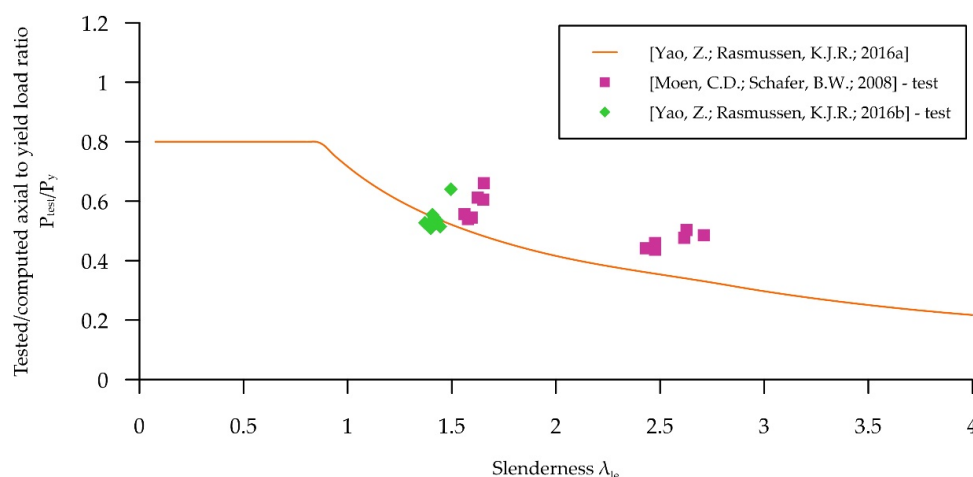


Figure 5. DSM prediction curves and experimental data for CFS columns predisposed to local buckling [2,11,12].

5. Bending

5.1. C-Section Beams

Extensive experimental research on the flexural, shear, and the combination of flexural and shear behaviour of CFS C-section elements with holes was conducted by Shan et al. [23]. The investigation stage of the flexural behaviour and strength was presented in [24]. Test specimens consisted of two connected simply supported C-section beams subjected to four-point bending test. Most of the specimens failed in local buckling, while some failed in the distortional. The bending resistance was mostly influenced by the web-opening-depth-to-web-flat-width ratio. Three different methods were examined for the determination of the moment capacity. The most accurate method was the effective net section approach, while the modification of the 1986 edition of AISI specification [110] using modified effective web area overestimated the bending resistance.

A somewhat different test setup was used by Shan et al. in [25], which was also one of the phases of the research presented in [23]. The interaction of flexural and shear behaviour showed that the local buckling around the hole and in the zone of load application was the governing failure mode. The ultimate resistance was evaluated by the use of the interaction equation incorporated in [110], and it was concluded that the predicted strength was accurate enough if the influence of the web holes was accounted for by the modification of the individual shear and bending capacities.

CFS C-section beams with rectangular web holes were experimentally tested by Moen et al. [29]. Test specimens consisted of two back-to-back connected beams. In each test, the failure first appeared in just one of the two beams. In most cases, distortional buckling with the maximum displacement at the hole was noticed, followed by unstiffened strip buckling of the compressed web above the hole. The unstiffened strip buckling was eliminated in cases where the hole depth was close to the web height. Nonetheless, an instantaneous local buckling of the compressed flange above the hole occurred. The flexural capacity of the tested specimens was compared to the one provided from the DSM equations of AISI S100-2007 [117]. Sufficient accuracy was achieved, although in some cases the ultimate capacity was underestimated.

The flexural behaviour, bending resistance, and failure modes of CFS members with circular web holes were investigated by Wang and Young [30]. Built-up beam specimens were subjected to a four-point bending test. Open and closed cross-section types were considered, as well as the influence of cross-section size and hole dimensions. It was discovered that the bending resistance decrease becomes more pronounced when the hole-diameter-to-web-height ratio exceeds the value of 0.5. The calculation of critical elastic local and distortional buckling moments was investigated through different approaches since the design equations in current design codes are intended to be applied only in cases

of a single beam. It was concluded that AISI S100-2012 is efficient in the prediction of the design strength of the built-up beams with holes.

In their following research [18], Wang and Young used the data previously collected in [30] to form an extensive parametric study on built-up sections. The parametric study included various section slenderness and hole sizes. Flexural resistance from the numerical analyses and test data from the previous research were compared to the calculated design resistances from AISI S100-2016. The DSM equations proved to be fairly accurate in the cases of open built-up sections with holes, whereas in cases of closed built-up sections with holes, the DSM equations were quite conservative. For this reason, modifications for the DSM equations for built-up closed section beams with holes were proposed.

The numerical and analytical study by Yuan et al. [19] dealt with the influence of the circular web holes on the distortional buckling of a mono-symmetric CFS C-section beams subjected to a uniform bending moment along its length. Numerical analyses were carried out by the use of a sophisticated FEM modelling tool, while an analytical model was established according to the recommendations provided in EN 1993-1-3. The compressed stiffened element (in this case, the flange) behaves as an elastically supported strut, since the lips of a channel section act as edge stiffeners. The spring stiffness along the length depended on the boundary conditions and the flexural stiffness of the adjacent plane elements of the cross-section. The decrease in the rotational stiffness of the web with regard to the compressed flange-lip element, caused by the introduction of web holes, could be introduced by the application of the proposed reduction factor. Additionally, although the increase in the hole size had reduced the distortional buckling moment, the half-wavelength associated to it had increased.

In their further research, Yu et al. [20] continued to study the influence of the circular web holes on the distortional buckling of the mono-symmetric CFS C-section beams. A detailed analytical study verified by FEM analyses revealed that the flange and lip system model presented by Hancock [26] (originally developed for members without holes) can be employed for the prediction of the distortional buckling stress of C-section beams with holes, provided that the rotational spring stiffness is correctly reduced. Furthermore, the proposed analytical method estimated the critical stress of the distortional buckling more accurately than the modified EN 1993-1-3 method [19]. The conclusion derived in [19] is in line with the one provided herein.

The flexural behaviour of CFS C-section beams with rectangular web holes was researched by experimental and numerical parametric analyses by Zhao et al. [21] in order to evaluate the reliability of the design method incorporated in AISI S100-2016. A four-point bending test was applied on test specimens with a wide range of hole and lip sizes. Specimens with shorter lips tended to buckle in a distortional–local mode interaction controlled by the distortional buckling, while those with longer lips were prone to failure in a local–distortional mode interaction controlled by the local one. Similarly to [30], the bending strength reduction became more apparent when the hole-height-to-web-depth ratio exceeded the value of 0.4. Experimental and FEM parametric results were compared to the DSM design predictions from AISI S100-2016. Modifications of the current design equations were necessary for beams which had exhibited failure in a local–distortional mode interaction controlled by local buckling, since the predicted design strengths lead to discrepancies compared to test results in a large number of specimens.

Numerical research by Moen and Schafer [3], mentioned in the previous section, had also covered the problems of the elastic buckling behaviour of beams with holes. As with columns, separate models are also needed in the case of beams for each type of elastic buckling, since the hole has a different influence on each buckling mode. The concept of “weighted average” cross-section properties for the approximation of flexural-torsional buckling load can also be extended to beams with holes. In addition, the principle of reduced thickness for the prediction of distortional buckling can be applied to beams as well. However, for the determination of local buckling load, only half-wavelengths smaller than the length of the hole are investigated in the net-section model.

Numerical research on the buckling behaviour of C-section beams with perforations of various shapes, sizes, numbers, spacing, and edge distances was carried out by Ling et al. [17]. Although a decrease in the buckling moment was expected with the introduction of web holes, it is worth mentioning that the lowest decrease was reported for a hexagon-shape opening.

5.2. C-Section Beams with Edge-Stiffened Web Holes

In order to limit the resistance reduction to as low as possible, hole edge stiffeners are introduced in beams. The previously discussed numerical research by Grey and Moen [4] examined the influence of hole edge-stiffening on the elastic buckling behaviour of beams as well. The concept of global, distortional, and local buckling load determination follows the same ideas as stated in [3] for members with unstiffened holes.

The behaviour and design of beams with edge-stiffened holes was studied and presented in detail by Yu [28]. FEM analyses were performed in order to investigate the elastic buckling of CFS thin plates and C-section beams with edge-stiffened holes. Critical buckling loads of thin plates with edge stiffeners, subjected to in-plane bending, were higher compared to plates without edge stiffeners. As the hole diameter became larger, the difference between the critical buckling loads was higher. The most efficient length of edge stiffener proved to be 0.06 times the plate width. Moreover, the shape of the first buckling mode was the same, regardless of the presence of the hole. Two different C-sections were analysed for member buckling. Sections were chosen in a manner such that one was prone to the local and the other to the distortional buckling. An increase in the buckling moment was recorded in cases of both local and the distortional buckling when edge-stiffened holes were introduced. Smaller spacing between holes influenced the increase in the buckling moment, since the longer spacing allowed the original lower buckling mode to occur in the area between holes, which means that the beam exhibited the same performance as the one without holes. Thus, the hole spacing of 305 mm proved to lead to optimal performance. Finally, the new design procedure based on the DSM was proposed for channel beams with optimized edge-stiffened holes.

With a similar test preparation as in [15], the same group of authors conducted a bending test on 14 back-to-back built-up channel specimens [22], of which 6 had edge-stiffened holes. Specimens with one, three, and five web holes were examined. As in their study on axial strength, members with edge-stiffened holes demonstrated a higher moment capacity by as much as 15.4%, while the capacity of the same section with un-stiffened holes was reduced by 15.1%, both compared to that of a plain channel. In all cases, members failed dominantly in the distortional buckling mode. Since the design equations provided by Moen and Schafer [3,29,100] were given for un-stiffened holes, they underestimated the moment capacities of specimens with edge-stiffened ones.

The first to introduce a machine learning model for purposes of prediction of the moment capacity of CFS members with web holes were Dai et al. [31]. They employed the XGBoost tool in order to develop the model. For the model to be trained, a number of FE models should be created and validated against experimental results in the existing literature. Further, a parametric study using the XGBoost model was conducted and a set of new design equations was proposed since the current design equations appeared to be unreliable for moment capacity calculation.

5.3. C-Section Beams with Web Reinforcement

Since the member resistance decreases noticeably when web holes are introduced, in addition to hole edge-stiffening, one of the methods to limit the decrease considers reinforcement of the hole itself.

Several different reinforcement schemes were experimentally tested by Sivakumaran et al. [118] on CFS C-section beams with web openings in order to determine the most adequate one. Test specimens consisted of two face-to-face connected beams subjected to a four-point bending test. Three groups of specimens were tested: a group without

web holes, one with a single web hole, and one with a single reinforced web hole, both positioned in the mid-span. Additionally, three different hole shapes were taken into account: circular, square, and rectangular. Specimens without holes failed due to local buckling of the compressed flange and compression in the web zone. The same character of failure could be observed in the members with holes, where it was observed that the local buckling occurs at the location of the opening. In addition, the bending capacity was reduced by approximately 10% compared to the members without holes. Two different hole reinforcement schemes were analysed. The reinforcement was beneficial in the zone close to the compression edges of the opening, whereas their location in the zone close to the tension edges was insignificant. Furthermore, screw fasteners of the reinforcement should be placed as close as possible. The bending capacity of the members with reinforced web holes was close to that of members without holes.

5.4. Comparison and Discussion

After design equations in compression were proposed and established, the research community turned to the design due to bending. Proposed design equations for elements in bending by various authors are outlined in Table A2 of Appendix A. Wang and Young [18] gave their proposal for built-up elements that fail in local buckling and Zhao et al. [21] modified it and added the group of equations for distortional buckling. For elements with edge-stiffened holes, Grey and Moen [4] provided provisions for lateral-torsional and distortional buckling, while a year later Yu [28] made his proposal for local buckling, which had a lot of similarities with the Wang's and Young's [18] solution.

In Figure 6, the prediction curves according to AISI S100-2016 for CFS beams predisposed to distortional buckling with and without holes are depicted, as well as the results of the experimental research conducted by Moen et al. [29] and Wang and Young [30]. In [29], the dominant form of failure was the distortional one. Nevertheless, local buckling of the compressed portion of the web at the hole was noticed on specimens with smaller holes. In [18], both back-to-back (open) and face-to-face (closed) section beams with circular holes were investigated. The governing failure modes of the specimens were not clearly separated, since all specimens exhibited a combination of flexural, distortional, and local buckling. The tests revealed that the DSM prediction curves in AISI S100-2016 for distortional buckling and elements of low slenderness yielded reliable results, while the bending resistance was underestimated for a small portion of specimens with slightly higher slenderness.

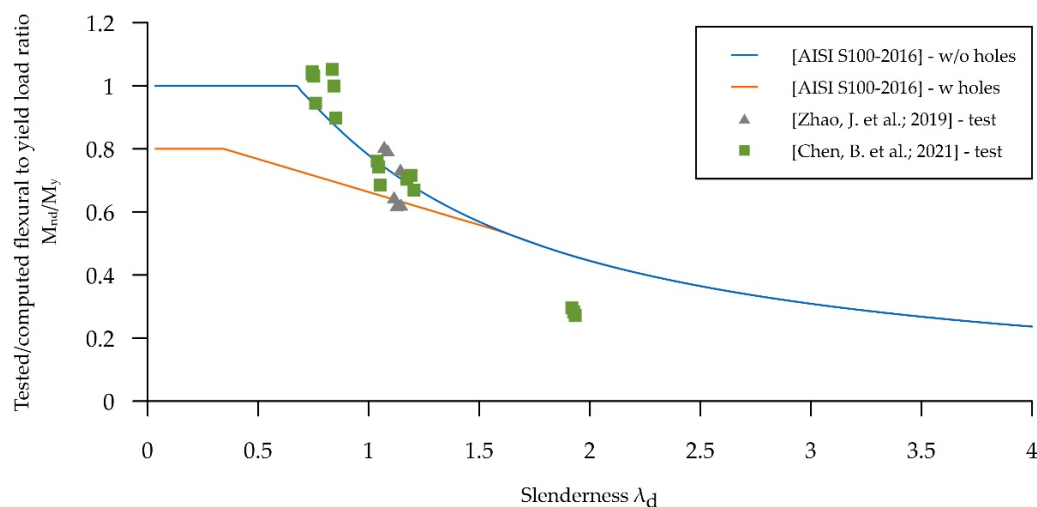


Figure 6. DSM prediction curves and experimental data for CFS beams predisposed to distortional buckling [21,22,89].

The DSM prediction curves according to [18,21,28,89] for elements prone to local buckling are given in Figure 7, as well as the experimental results of the same authors shown in Figure 6. All design equations are given for the same yield moment of net cross-section-to-yield-moment-of-gross-cross-section ratio $M_{yn}/M_y = 0.8$. The exception is the design equation for elements with edge-stiffened holes, introduced in [28], which does not account for the aforementioned ratio. For the elements of low slenderness, the equation given in [17] proved to be the most fitting, while for elements with higher slenderness, AISI S100-2016 turned out to be the most appropriate.

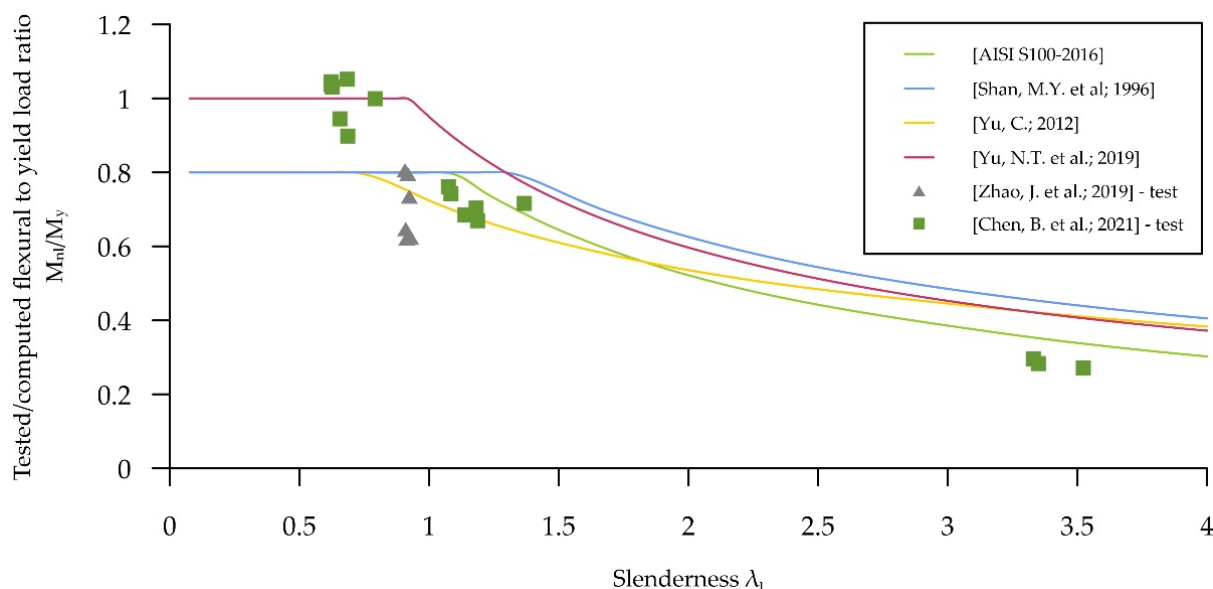


Figure 7. DSM prediction curves and experimental data for CFS beams predisposed to local buckling [20–22,25,28,89].

6. Web Crippling

6.1. C-Sections

As a result of their usually slender web, CFS flexural members are prone to web crippling due to high local stress concentration. Moreover, the presence of holes along the web may result in enhanced susceptibility to such effects, especially if the holes are located in the vicinity of the support or the location of the concentrated load.

In their comprehensive research, apart from the investigation on the buckling of compressed elements, Davis and Yu [59] also studied the crippling strength of members with web holes. Test specimens were built-up face-to-face and back-to-back C-sections without lips subjected to the interior-two-flange (ITF) loading condition. The reduction factors for the modification of the AISI [119] design equations were proposed to take into account the effect of circular and square web holes.

Besides the stub column tests, Sivakumaran [109] also carried out web crippling tests on 55 interior-one-flange (IOF) loaded C-section specimens with various hole shapes and sizes. The study found that the 1984 edition Canadian CFS design code [120] yielded about 15% lower web crippling strength compared to experimental.

The same conclusion was derived from the experimental investigation by Sivakumaran and Zielonka [60]. In addition, the web hole height has a more pronounced influence than its length. Moreover, an equation for the web crippling strength reduction factor was proposed to account for the influence of web openings.

During the 1990s, several studies were carried out in the Center for Cold-Formed Steel Structures at the University of Missouri-Rolla. The specimens comprised two back-to-back connected C-sections. The first and the most detailed study was carried out by Langan et al. [61], considering unreinforced and reinforced specimens subjected to the end-

one-flange (EOF) and IOF loading conditions. Since the web crippling provisions of the 1986 edition of AISI Specifications [110] were incapable of predicting the web crippling strength of members with web holes, design recommendations were provided. Reduction factor equations were derived for the EOF and IOF cases, and provisions for web reinforcement were given. Extensions to this research were provided by Deshmukh et al. [62] and Uphoff et al. [63]. LaBoube et al. [47] presented a brief summary of the previous studies and drew out the most important conclusions.

Uzzaman et al. [48] conducted experimental research on C-section members with various sizes of circular web holes subjected to ITF loading conditions, in which the load was not applied directly above the hole. The influence of the fastening of flanges to the bearing plates was also considered. Test results were used to validate FEM models, followed by a parametric study. The leading factors for the web crippling strength decrease were hole-to-web-depth ratio and the clear-distance-from-hole-to-the-bearing-plate-to-web-depth ratios. Finally, reduction factors were proposed for the ITF loading condition.

A similar investigation carried out by Uzzaman et al. [49,50] considered both end-two-flange (ETF) and ITF loading conditions. However, in this case the hole was located directly under the concentrated load. The tests and FEM analyses were conducted on 82 specimens, followed by a numerical parametric investigation, which led to the same conclusion as in [48]. The equations for web crippling strength reduction factors for both ITF and ETF loading conditions for the cases of unfastened and fastened flanges to the support were proposed. In a further study on the web crippling strength of C-sections subjected to the ETF loading condition by Uzzaman et al. [51], similar conclusions as in [48] regarding the web crippling strength reduction factors were outlined.

The web crippling behaviour and strength of the CFS elements with holes subjected to the end-one-flange (EOF) loading condition was investigated by Lian et al. [52,53]. A total of 74 specimens were tested (52 with and 22 without web holes). Test specimens comprised a pair of C-sections with holes of variable dimensions, centred above the bearing plate or offset from it. In addition to the experimental testing, parametric numerical analyses were performed. Web crippling behaviour was mostly influenced by the following ratios: hole to web depth; bearing plate length to web depth; and clear distance from hole to the bearing plate to web depth. Modifications of the design equations given in AISI S100-2016 for web crippling strength reduction factors for the EOF loading condition for the cases of unfastened and fastened flanges to the support were proposed. The web crippling behaviour under the IOF loading condition was studied in a similar manner by the same authors [54,55].

A similar procedure as described in [49,50], but on ferritic stainless CFS channel sections without lips subjected to the ITF loading condition, was employed in the research by Yousefi et al. [57,58], which also proposed the design equations for the web crippling strength reduction factors.

6.2. C-Sections with Edge-Stiffened Web Holes

The influence of hole edge-stiffening on the web crippling strength of CFS C-sections under IOF and EOF loading conditions was investigated by Uzzaman et al. [33]. Experimental tests were carried out on three groups of 12 specimens: plain sections, sections with unstiffened holes, and sections with edge-stiffened holes. The consequent parametric study explored the influence of web slenderness and hole diameter. The reduction of web crippling strength was up to 12% and 28%, for the IOF and EOF loading conditions, respectively, for the case of unstiffened holes. For the case of edge-stiffened holes, the strength decrease was only 3% for the IOF loading condition, while there was no strength decrease for the EOF loading condition.

The next phase of the experimental testing was to apply the ETF [34] and ITF [35] loading conditions. Both studies were carried out by Uzzaman et al. on 30 web crippling tests, which were accompanied by extensive FEM parametric analysis. It was revealed that the member web crippling strength decrease was minimal, while in some cases it was

even improved. In their further experimental and numerical research [36], specimens with fastened flanges demonstrated higher web crippling capacity.

6.3. Comparisons and Discussion

Web crippling of a thin-walled sections is a phenomenon that, in the field of CFS members with holes, has been dealt with for as long as a half a century. Since Davis and Yu [59] proposed equations for web crippling strength reduction factors as functions of the hole-size-to-web-flat-height ratio (d/h), most of the following researchers followed their course. As researchers became more familiar with the web crippling behaviour, more variables were added to design equations. During the past decade in particular, a great effort was put in to develop the most suitable reduction factor equations. However, the essence of the equations remained the same in all research, only with variations in values of numerical constants. In Table A3 of Appendix A, the proposed design equations for CFS members with web holes subjected to web crippling are outlined.

In Figures 8–11, the comparison of the web crippling reduction factors (R_p) in the function of the d/h ratio proposed by various authors is depicted. Other variables in proposed equations were considered to be constant and same for all cases. Proposed curves are presented for different loading and boundary conditions and different positions of the web holes. Additionally, the relevant experimental results are outlined. In these figures, a set of abbreviations is used: CH (centred holes), OH (offset holes), UF (unfastened flanges), FF (fastened flanges), USH (unstiffened holes), ESH (edge-stiffened holes).

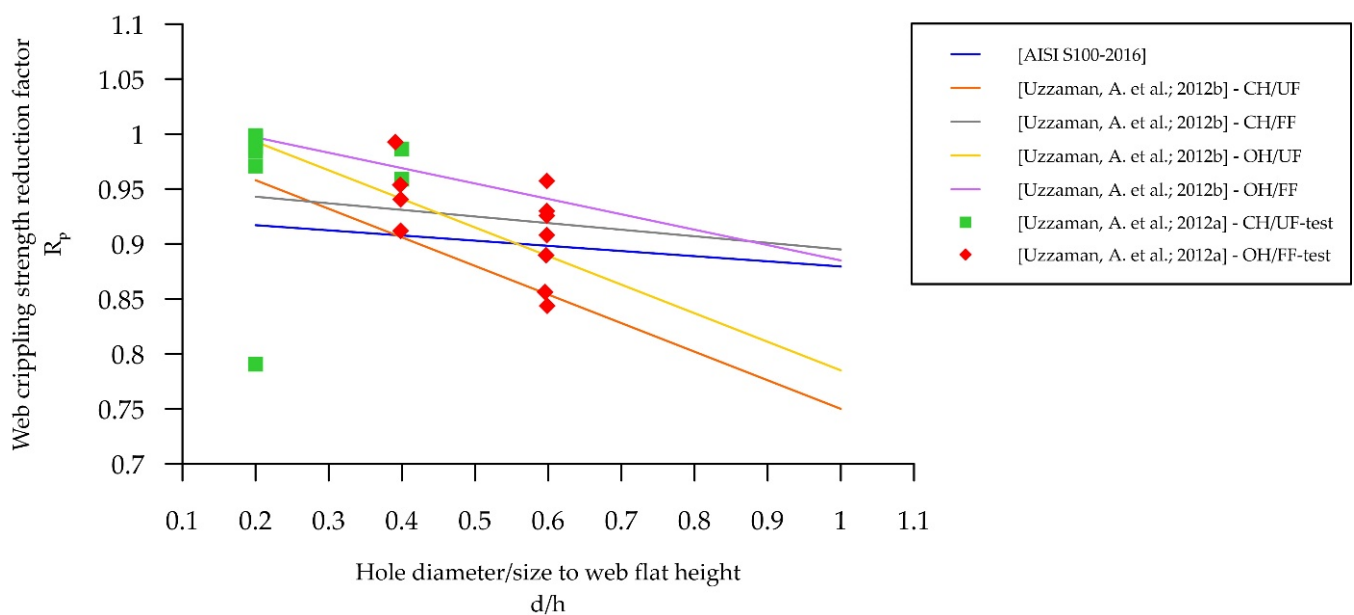


Figure 8. Proposed reduction factor curves and experimental data for CFS elements subjected to web crippling due to IOF loading [48,49,89].

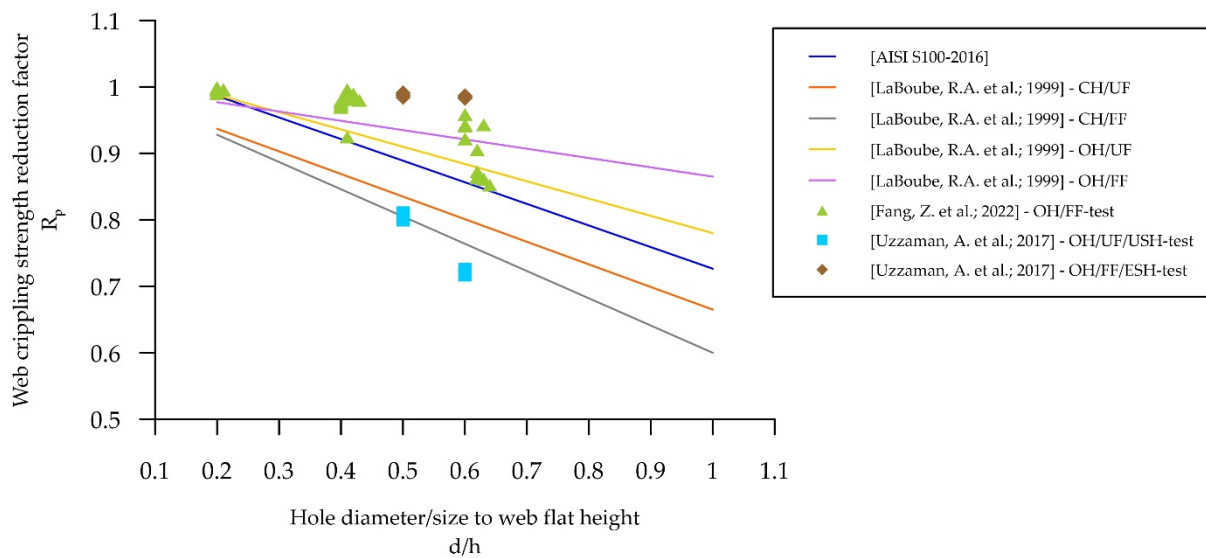


Figure 9. Proposed reduction factor curves and experimental data for CFS elements subjected to web crippling due to EOF loading [33,47,65,89].

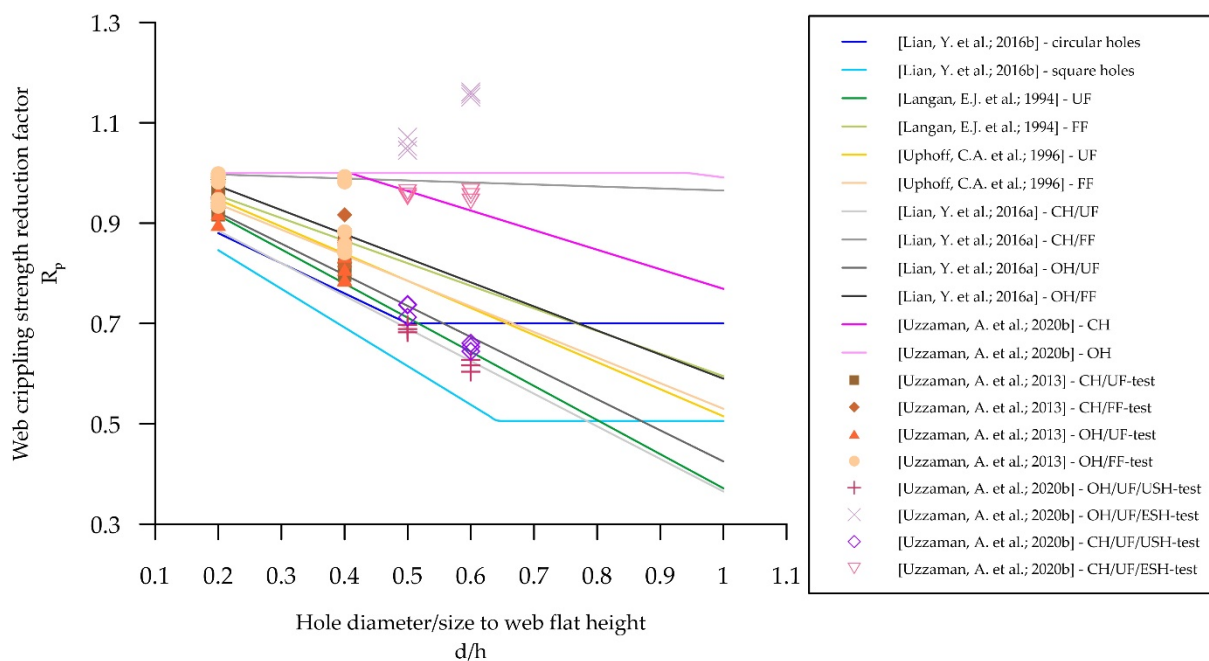


Figure 10. Proposed reduction factor curves and experimental data for CFS elements subjected to web crippling due to ITF loading [35,51–53,61,63].

In case of IOF loading, the decrease in the reduction factor is gradual, which means that the d/h ratio does not greatly influence the web crippling strength. An experimental study conducted by Lian et al. [54,55] showed that a significant decrease in bearing capacity can be expected in cases of unstiffened flanges. Based on the experimental research conducted by Lian et al. [52,53] and their proposed equations for the EOF loading cases, it can be concluded that the configurations with the offset holes showed the highest web crippling resistance, unlike the ones with the centred holes. In both cases, the equation proposed in AISI S100-2016 is intended for use in cases within the prescribed provisions.

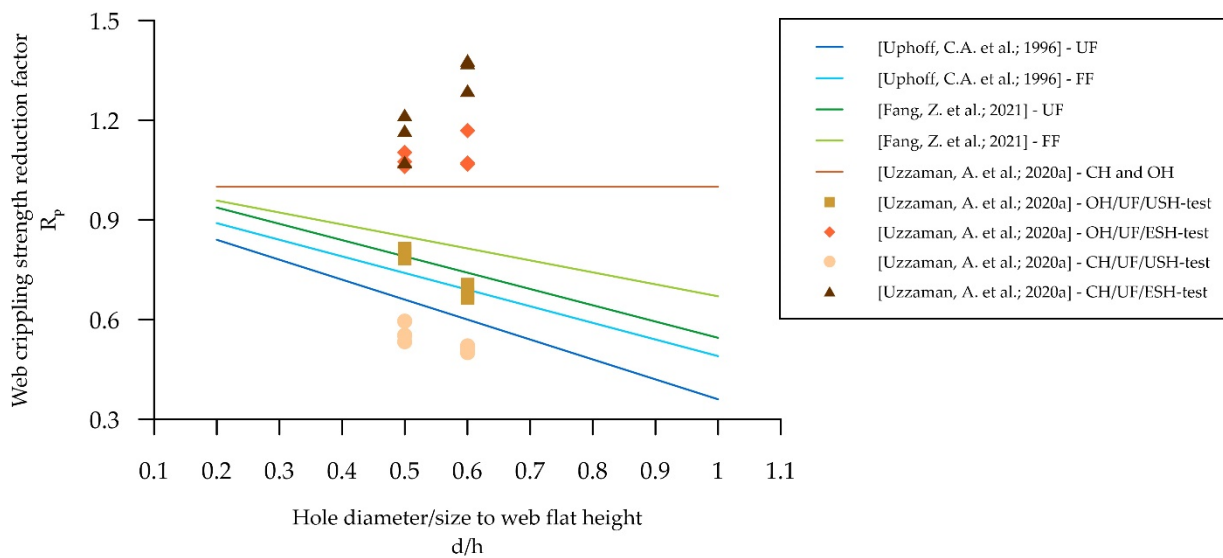


Figure 11. Proposed reduction factor curves and experimental data for CFS elements subjected to web crippling due to ETF loading [34,63,64].

The most examined case of the web crippling is the case of ITF loading. The web crippling strength decrease was more rapid in comparison to the one-flange loading, which might be caused by the high-intensity local stresses in the vicinity of both sides of the holes.

As in the case of interior-flange loading, the web crippling strength due to the end-flange loading decreases at a faster rate in the case where both flanges are loaded with a concentrated load.

In all cases in which experimental testing was performed on elements with edge-stiffened holes, it was shown that the hole stiffening had a favourable effect on the web crippling strength, i.e., no decrease in load-bearing capacity was observed in relation to the elements without holes.

7. Shear

7.1. C-Sections

The behaviour of a C-section with web openings and a linearly varying shear force was investigated by Eiler et al. [66]. Experimental testing was conducted on a total of 46 test specimens with circular, elliptical, and diamond-shaped holes. Design equations were proposed for the reduction factors that are applied to the shear strength of the same beams without web holes.

In recent years, a group of researchers at the University of Sydney led by Gregory J. Hancock has been investigating the influence of web holes on the behaviour of single CFS members subjected to shear. The effect of circular and square web holes on the buckling behaviour of thin-walled plates and CFS C-sections was numerically investigated by C.H. Pham [43]. The solutions of the Spline Finite Strip Method (SFSM) [121] were utilised. Three load distribution cases for the C-section were investigated, while on the plate only uniform distribution was taken into consideration. It was found that, for small web openings, shear buckling coefficients were only slightly reduced compared to the cases without web holes. A considerable difference in shear buckling coefficients was calculated when the holes were larger. Additionally, the influence of the bending moment applied at one or both ends of the section was negligible. Design equations were proposed for the approximation of the shear buckling coefficients for square plates and C-sections.

Shear experimental testing on 40 C-section specimens with circular web holes was carried out by Keerthan and Mahendran [67]. Simply supported specimens consisted of two bolted back-to-back sections, with and without straps, subjected to a mid-span loading (three-point test). Since short beams without straps experienced combined shear

and flange distortion action, the distortion of the flange occurred as a result of distortional buckling. Shear strength was compared to that predicted in the 2005 edition of AS/NZS 4600 [122] and by LaBoube et al. [123]. Since the predictions were either too conservative or unreliable, enhanced design equations were proposed. In their following study, Keerthan and Mahendran [68] conducted a numerical investigation and extensive parametric analysis based on the previously published experimental results and conclusions.

S.H. Pham [44] studied shear buckling and shear strength of CFS C-section members with web holes and with or without intermediate transverse web stiffeners. The experimental investigation and the strategy for a new approach of the DSM design in which the Vierendel mechanism [124] is recognised are summarised in [69–71]. Test specimens included two bolted back-to-back C-section beams with a shear-span-to-web-depth ratio (aspect ratio—AR) of 2.0. Web depth and shear span were 200 and 400 mm, respectively. Since, at this aspect ratio, the ultimate state is controlled by bending, in order to isolate the shear failure mode, dual actuator testing equipment was used. Circular holes with diameters ranging from 50 to 145 mm and square holes with sizes from 40 to 120 mm were taken into account. As expected, the shear strength decrease became more pronounced with larger holes and a failure occurred in a proximity of the hole. Furthermore, it was revealed that the design provisions in the specification for structural steel buildings [125] were reliable, contrary to the ones provided by AISI S100-2016, which appeared to be overly conservative.

The extension of the previous research carried out by D.K. Pham et al. [45] on 30 C-section specimens with ARs of 1.0, 2.0, and 3.0 and with different sizes of square, rectangular, circular, and industrially slotted web holes included the same dual actuator test rig as in [44]. It was found that the current DSM design method was reliable for the design of sections with a hole size up to 80×240 mm, and a new proposal for the DSM design of shear members with elongated web holes that relies on the Vierendeel mechanism approach was presented.

Based on the previous research, D.K. Pham et al. [72] conducted an FEM parametric investigation for a better understanding of the previous conclusions.

Experimental research by C.H. Pham and Hancock [46] was carried out with the aim to develop a new, simplified equation for shear yielding load (V_y), which is one of the required inputs in the DSM shear design equations. A total number of 24 C-section specimens with a web depth of 200 mm, variable thickness, and square web holes (40×40 mm, 80×80 mm, and 120×120 mm) were tested, followed by an FEM parametric analysis, varying the section thickness and hole size.

7.2. C-Section Beams with Web Reinforcement

The influence of web hole reinforcement in a high-shear zone was also experimentally investigated on built-up CFS beams by Acharya et al. [73]. Test specimens were subjected to a mid-span concentrated load. As in [118], the same three groups of specimens were considered. Circular and square web holes with a height of about 65% of the web depth were taken into account. Three reinforcement schemes were considered. Scheme A, considering solid plate reinforcement around the holes, could not adequately improve the shear strength of the section, while scheme B, in the form of joist section reinforcement in the zone of the hole, could be used only to reinforce the circular web opening. However, reinforcement scheme C, consisting of bridging channels around the hole, proved to be the most suitable to overcome the shear effects due to two reasons: (i) the failure mode shape of specimens with the reinforcement scheme C closely resembles the members without holes, and (ii) the shear resistance was higher compared to the members without holes.

7.3. Comparisons and Discussion

Design equations for elements in shear proposed by various authors are outlined in Table A4 of Appendix A. Namely, two different concepts can be recognised. Eiler et al. [66] gave a proposition for the calculation of reduction factors which were later multiplied with

the shear resistance of members without web holes. Their concept was later adopted and simplified by Keerthan and Mahendran [67]. Several years later, S. H. Pham [44] introduced an approach in which the shear resistance of a member with web holes is determined directly by taking into account the cross-sectional and hole properties. A similar idea was also recognised in the work of D. K. Pham et al. [45].

In Figure 12, the comparison of the shear strength reduction factor as a function of the hole-diameter-to-flat-portion-of-the-web ratio (d/h) is depicted. Design equations presented in AISI S100-2016 are proposed for the circular and non-circular hole shape, while the experimental research in [124] was conducted on CFS elements with only circular holes. In [67], specimens with and without horizontal reinforcing straps on the compressed flange were investigated and two design equations were presented. Specimens without straps exhibited deformation as a combination of the shear and distortional forms. This was caused by distortional buckling of the compressed flange and unbalanced shear flow. It was proven that the design equation suggested in AISI S100-2016 overestimated the shear strength of members with circular holes, which was more pronounced in cases of larger hole diameters. Although it may seem that the deviations in the equations are significant for the d/h ratio greater than 0.4, the proposed curves are fairly suitable for the appropriate experimental data.

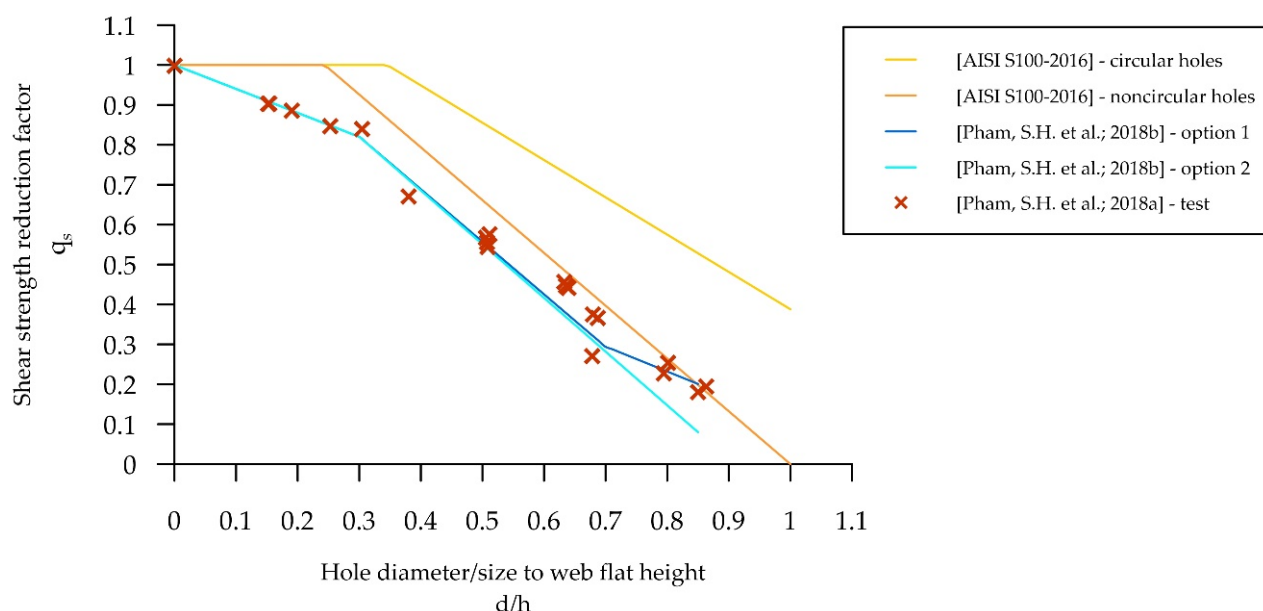


Figure 12. Proposed reduction factor curves and experimental data for CFS elements subjected to shear [69,70,89].

8. Conclusions

The growing trend in the use of CFS members with web holes and the importance of their optimisation imposes the need for extensive experimental research. The greatest progress in research was achieved during the previous decade, on the grounds of the advancement of numerical methods and their capabilities to capture the complex behaviour of thin-walled members. In this paper, a summary of the current leading design codes for CFS members with web holes and main concepts of design, as well as an outline of the accompanying numerical solutions, was briefly described. The experimental tests, numerical simulations, and design proposals are outlined for pure compression, bending, web crippling, and shear.

As presented in the review, numerous design equations were suggested in order to take into account the effects of the web holes on CFS columns and beams. However, to date, there is neither consensus nor uniformity in the proposed design equations and approaches. Currently, only North American and Australian/New Zealand design codes

incorporate the calculation of CFS elements with web holes and offer certain guidelines. Further development of the design codes in this field is undoubtedly dependent on future research and reaching a firm consensus in the design approach. An additional difficulty is the fact that different design codes are fundamentally different in terms of approach and the calculation of CFS elements, in general. Therefore, the intent of this paper is to thoroughly present the up-to-date research, both experimental and numerical, and to compare the proposed design procedures.

Although the research carried out so far on CFS members with web holes has been thorough, further investigations are required. A commonly occurring case in the engineering practice of combined compression and bending should attract more attention from researchers.

The experimental results for columns prone to local buckling indicate that the tests were conducted on members with slenderness factors for local buckling of around 1.5 and 2.5. Therefore, experimental testing should be extended to members with different slenderness values. For beams prone to distortion and local buckling, most of the results are obtained for beams with slenderness factors of around 1.0; thus, the area of greater slenderness should be studied. In addition, the influence of the hole position along the element, as well as the effect of the imperfections on the member resistance, should be examined in more detail.

Author Contributions: Conceptualization, methodology, V.Ž.; Đ.J., D.K. and I.D.; investigation, V.Ž.; resources, Đ.J.; writing—original draft preparation, V.Ž. and Đ.J.; writing—review and editing, V.Ž. and I.D.; visualization, V.Ž. and I.D.; supervision, D.K.; project administration, D.K. and I.D. All authors have read and agreed to the published version of the manuscript.

Funding: This research has been supported by the Ministry of Education, Science and Technological Development through project No. 451-03-68/2022-14/200156 “Innovative scientific and artistic research from the FTS (activity) domain”.

Conflicts of Interest: The authors declare no conflict of interest.

Nomenclature

A_0	gross cross-section area
A_f	flange area
A_h	hole area
A_s	area of the opening
A_w	web area
b	horizontal width of a rectangular opening
$C_{w,net}$	warping stiffness of the net section
d	circular hole diameter or the square hole size
E	Young’s modulus of elasticity
EI_{web}	flexural stiffness of the web
GJ_f	torsional stiffness of the rectangular hollow flange
h	flat height of the web
h_s	web stiffener height
I_g	moment of inertia of the gross cross section
I_{net}	moment of inertia of the net cross-section at a hole
J_{avg}	St. Venant torsional constant including the influence of holes
k_0	shear buckling coefficient of the member without the hole
k_v	shear buckling coefficient for the member with the hole
L	member length/span ($L_g + L_{net}$)
L_g	length of the portion of column without holes
L_{net}	length of the portion of column with holes

M_{crd}	critical elastic distortional buckling moment
M_{crd-h}	critical elastic distortional buckling moment including the influence of holes
M_{crd-nh}	critical elastic distortional buckling moment without the influence of holes
M_{cre-h}	critical elastic lateral–torsional buckling moment including the influence of holes
M_{crl-h}	critical elastic local buckling moment including the influence of holes
M_{crl-nh}	critical elastic local buckling moment without the influence of holes
M_{nd}	nominal flexural strength for distortional buckling
M_{ne}	nominal flexural strength for lateral–torsional buckling
M_{nl}	nominal flexural strength for local buckling
M_{pv}	plastic bending moment capacity of the top (or bottom) segment above (or below) the opening (including the flanges and the lips)
M_u	nominal flexural strength
M_y	member yield moment
M_{yn}	member yield moment of net cross-section
N	length of bearing plate
n	effective length of the load (support) plate
P_{crd}	critical elastic buckling load for distortional buckling
P_{crd-h}	critical elastic buckling load for distortional buckling for member with holes
P_{crd-nh}	critical elastic buckling load for distortional buckling for member without holes
P_{cre-h}	critical elastic buckling load for global buckling for member with holes
P_{crl}	critical elastic buckling load for local buckling
P_{crl-h}	critical elastic buckling load for local buckling for member with holes
P_{crl-nh}	critical elastic buckling load for local buckling for member without holes
P_{MS}	compression resistance of the member with web holes predicted from [5]
P_{nd}	nominal axial resistance for distortional buckling
P_{ne}	nominal axial resistance for overall buckling
P_{nle}	nominal axial resistance for local buckling
P_{prop}	compression resistance of the member with web holes
P_{ult}	compression resistance of the member with web holes
P_y	axial yield load
P_{yn}	member yield strength on net cross-section
q	length of the web hole’s edge-stiffener
q_s	shear strength reduction factor
R_p	proposed web crippling strength reduction factor
r_q	inside corner radius between the web and the hole’s edge-stiffener
S	hole spacing
s	clear hole spacing
t	web thickness
t_{equ}	equivalent thickness
t_f	flange thickness
V_1, V_2	shear forces at each edge of the hole
V_n	nominal shear resistance per web in accordance with [126]
V_{nl}	reduced shear capacity for a member with a hole
V_v	shear capacity for the member without the hole
V_{vrd}	shear carried out over the opening based on the Vierendel mechanism
$V_{vrd,0.6}$	shear carried out over the opening based on the Vierendel mechanism calculated for the member with holes with the ratio $d/h = 0.6$
$V_{vrd,m}$	shear carried out over the opening based on the Vierendel mechanism calculated for the member with holes with the ratio $dh/h = m$
V_y	yield shear load for the member without holes
V_{yh}	yield shear load for the member with holes
x	horizontal clear distance of web holes to the bearing plate edge

Appendix A

Tables A1–A4 present a summary of the proposed designed equations for different stress states according to various authors.

Table A1. Design equations in pure compression.

Reference	Equation	Note
Shanmugam and Dhanalakshmi [40]	$\frac{P_{ult}}{P_y} = k_1 \left(\frac{A_0}{A_1} \right) + k_2 \left(\frac{A_0}{A_1} \right)^{0.5} + k_3$ $k_1 = 1.1850m^3 - 3.8487m^2 + 3.7321m - 1.2336$ $k_2 = 0.1111m^2 + 0.0932m - 0.7763$ $k_3 = 0.11m^2 - 0.5681m + 1.1412$ $m = \frac{1}{100} \cdot \frac{h}{t}$	
	$P_{ne} = (0.658\lambda_c^2) P_y, \text{ for } \lambda_c \leq 1.5$ $P_{ne} = \left(\frac{0.877}{\lambda_c^2} \right) P_y, \text{ for } \lambda_c > 1.5$ $\lambda_c = \sqrt{\frac{P_y}{P_{cre-h}}}$	flexural, torsional or torsional–flexural buckling
Moen and Schafer [5], design option 4	$P_{nle} = P_{ne} \leq P_{yn}, \text{ for } \lambda_{le} \leq 0.776$ $P_{nle} = \left[1 - 0.15 \left(\frac{P_{crd-h}}{P_{ne}} \right)^{0.4} \right] \left(\frac{P_{crd-h}}{P_{ne}} \right)^{0.4} P_{ne} \leq P_{yn}, \text{ for } \lambda_{le} > 0.776$ $\lambda_{le} = \sqrt{\frac{P_{ne}}{P_{crd-h}}}$	local buckling
	$P_{nd} = P_{yn}, \text{ for } \lambda_d \leq \lambda_{d1}$ $P_{nd} = P_{yn} - \left(\frac{P_{yn} - P_{d2}}{\lambda_{d2} - \lambda_{d1}} \right) (\lambda_d - \lambda_{d1}), \text{ for } \lambda_{d1} < \lambda_d \leq \lambda_{d2}$ $P_{nd} = \left[1 - 0.25 \left(\frac{P_{crd-h}}{P_y} \right)^{0.6} \right] \left(\frac{P_{crd-h}}{P_y} \right)^{0.6} P_y, \text{ for } \lambda_d > \lambda_{d2}$ $\lambda_d = \sqrt{\frac{P_y}{P_{crd-h}}}, \lambda_{d1} = 0.561 \left(\frac{P_{yn}}{P_y} \right), \lambda_{d2} = 0.561 \left[14 \left(\frac{P_y}{P_{yn}} \right)^{0.4} - 13 \right]$ $P_{d2} = \left[1 - 0.25 \left(\frac{1}{\lambda_{d2}} \right)^{1.2} \right] \left(\frac{1}{\lambda_{d2}} \right)^{1.2} P_y$	distortional buckling
	$P_{ne} = (0.658\lambda_c^2) P_y, \text{ for } \lambda_c \leq 1.5$ $P_{ne} = \left(\frac{0.877}{\lambda_c^2} \right) P_y, \text{ for } \lambda_c > 1.5$ $\lambda_c = \sqrt{\frac{P_y}{P_{cre-h}}}$	flexural, torsional or torsional–flexural buckling
Yao and Rasmussen [12], proposed method 1	$P_{nle} = P_{ne} \leq P_{yn}, \text{ for } \lambda_{le} \leq 0.776$ $P_{nle} = \left[1 - 0.15 \left(\frac{P_{crd-nh}}{P_{ne}} \right)^{0.4} \right] \left(\frac{P_{crd-nh}}{P_{ne}} \right)^{0.4} P_{ne} \leq P_{yn}, \text{ for } \lambda_{le} > 0.776$ $\lambda_{le} = \sqrt{\frac{P_{ne}}{P_{crd-nh}}}$	local buckling
	$P_{nd} = P_{min}, \text{ for } \lambda_d \leq \lambda_{d1}$ $P_{nd} = P_{min} - \left(\frac{P_{min} - P_{d2}}{\lambda_{d2} - \lambda_{d1}} \right) (\lambda_d - \lambda_{d1}), \text{ for } \lambda_{d1} \leq \lambda_d \leq \lambda_{d2}$ $P_{nd} = \left[1 - 0.25 \left(\frac{P_{crd-nh}}{P_{ne}} \right)^{0.6} \right] \left(\frac{P_{crd-nh}}{P_{ne}} \right)^{0.6} P_{ne}, \text{ for } \lambda_d > \lambda_{d2}$ $\lambda_d = \sqrt{\frac{P_{ne}}{P_{crd-nh}}}, \lambda_{d1} = 0.561 \left(\frac{P_{yn}}{P_y} \right), \lambda_{d2} = 0.561 \left[14 \left(\frac{P_y}{P_{yn}} \right)^{0.4} - 13 \right]$ $P_{d2} = \left[1 - 0.25 \left(\frac{1}{\lambda_{d2}} \right)^{1.2} \right] \left(\frac{1}{\lambda_{d2}} \right)^{1.2} P_{ne}, P_{min} = \min(P_{ne}, P_{yn})$	distortional buckling
Chen et al. [14] (columns with edge-stiffened holes)	$P_{prop} = 1.92 \left(\frac{q}{s} \right)^{0.047} \cdot \left(\frac{r_q}{s} \right)^{0.017} \cdot P_{MS}, \text{ for } 0.28b < \lambda_c < 0.77b$ $P_{prop} = 1.95 \left(\frac{q}{s} \right)^{0.034} \cdot \left(\frac{r_q}{s} \right)^{0.022} \cdot P_{MS}, \text{ for } 0.77b < \lambda_c < 1.71b$ $P_{prop} = 1.91 \left(\frac{q}{s} \right)^{0.038} \cdot \left(\frac{r_q}{s} \right)^{0.021} \cdot P_{MS}, \text{ for } 1.71b < \lambda_c < 2.68b$ $\lambda_c = \sqrt{\frac{P_y}{P_{cre-h}}}$	

Table A1. Cont.

Reference	Equation	Note
Grey and Moen [4] (columns with edge-stiffened holes)	$P_{cre-h} = \frac{\pi^2 E}{L^2} \left(\frac{I_g L_g + I_{net} L_{net}}{L} \right)$	global flexural buckling
	$P_{cre-h} = \frac{A_0}{2\beta} \left[(\sigma_{ex} + \sigma_t) - \sqrt{(\sigma_{ex} + \sigma_t)^2 - 4\beta\sigma_{ex}\sigma_t} \right]$	flexural–torsional buckling
	$P_{crd} = \min(P_{crd-nh}, P_{crd-h})$	distortional buckling
	$P_{crl} = \min(P_{crl-nh}, P_{crl-h})$	local buckling

Table A2. Design equations in bending.

Reference	Equation	Note
Wang and Young [18]	$M_{nl} = M_{yn}, \text{ for } \lambda_l \leq 0.936$ $M_{nl} = \left[1 - 0.04 \left(\frac{M_{crl-h}}{M_y} \right)^{0.32} \right] \left(\frac{M_{crl-h}}{M_y} \right)^{0.32} \cdot M_y \leq M_{yn}, \text{ for } \lambda_l > 0.936$ $\lambda_l = \sqrt{\frac{M_y}{M_{crl-h}}}$	built-up sections, local buckling
Zhao et al. [21]	$M_{nl} = M_{yn}, \text{ for } \lambda_l \leq \lambda_a$ $M_{nl} = \alpha \left[1 - 0.15 \left(\frac{M_{crl-h}}{M_{ne}} \right)^{0.4\beta} \right] \left(\frac{M_{crl-h}}{M_{ne}} \right)^{0.4\beta} \cdot M_{ne} \leq M_{yn}, \text{ for } \lambda_l > \lambda_a$ $\alpha = \left(\frac{M_{yn}}{M_y} \right)^{19.4 \left(\frac{M_{yn}}{M_y} \right) - 14.8}, \beta = \left(\frac{M_{yn}}{M_y} \right)^{2.1}, \lambda_l = \sqrt{\frac{M_y}{M_{crl-h}}}, \frac{\alpha \left(1 - \frac{0.15}{\lambda_a^{0.8\beta}} \right)}{\lambda_a^{0.8\beta}} = \frac{M_{yn}}{M_y}$	local buckling
	$M_{nd} = M_{yn}, \text{ for } \lambda_d \leq \lambda_{d1}$ $M_{nd} = M_{yn} - \left(\frac{M_{yn} - M_{d2}}{\lambda_{d2} - \lambda_{d1}} \right) (\lambda_d - \lambda_{d1}) \leq$ $\leq 0.88 \left[1 - 0.2 \left(\frac{M_{crl-h}}{M_y} \right)^{0.45} \right] \left(\frac{M_{crl-h}}{M_y} \right)^{0.45} \cdot M_y, \text{ for } \lambda_{d1} < \lambda_d \leq \lambda_{d2}$ $M_{nd} = 0.88 \left[1 - 0.2 \left(\frac{M_{crl-h}}{M_y} \right)^{0.45} \right] \left(\frac{M_{crl-h}}{M_y} \right)^{0.45} \cdot M_y, \text{ for } \lambda_d > \lambda_{d2}$ $\lambda_d = \sqrt{\frac{M_y}{M_{crl-h}}}, \lambda_{d1} = 0.538 \left(\frac{M_{yn}}{M_y} \right)^3, \lambda_{d2} = 0.538 \left[1.7 \left(\frac{M_y}{M_{yn}} \right)^{2.7} - 0.7 \right],$ $M_{d2} = 0.88 \left[1 - 0.2 \left(\frac{1}{\lambda_{d2}} \right)^{0.9} \right] \left(\frac{1}{\lambda_{d2}} \right)^{0.9} \cdot M_y$	distortional buckling
Grey and Moen [4] (beams with edge-stiffened holes)	$M_{cre-h} = \frac{\pi}{L} \sqrt{EI_{y,avg} \left(GJ_{avg} + EC_{w,net} \frac{\pi^2}{L^2} \right)}$ $M_{crd} = \min(M_{crd-nh}, M_{crd-h})$	lateral–torsional buckling distortional buckling
Yu [28] (beams with edge-stiffened holes)	$M_{nl} = M_y, \text{ for } \lambda_l \leq 0.925$ $M_{nl} = \left[1 - 0.05 \left(\frac{M_{crl-nh}}{M_y} \right)^{0.35} \right] \left(\frac{M_{crl-nh}}{M_y} \right)^{0.35} \cdot M_y, \text{ for } \lambda_l > 0.925$ $\lambda_l = \sqrt{\frac{M_y}{M_{crl-nh}}}$	local buckling

Table A3. Design equations in web crippling.

Reference	Equation	Note
Davis and Yu [59]	for circular holes: $R_p = \left(1 - 0.6\frac{d}{h}\right)$, for $0 < \frac{d}{h} \leq 0.5$	ITF
	for square holes: $R_p = \left(1 - 0.77\frac{d}{h}\right)$, for $0 < \frac{d}{h} < 0.642$	
Uzzaman et al. [48]	for unfastened flanges: $R_p = 1.04 - 0.68\left(\frac{d}{h}\right) + 0.023\left(\frac{x}{h}\right) \leq 1$	ITF
	for fastened flanges: $R_p = 1 - 0.45\left(\frac{d}{h}\right) + 0.09\left(\frac{x}{h}\right) \leq 1$	
Uzzaman et al. [50]	for unfastened flanges: $R_p = 1.05 - 0.54\left(\frac{d}{h}\right) + 0.01\left(\frac{N}{h}\right) \leq 1$	ITF
	for fastened flanges: $R_p = 1.01 - 0.51\left(\frac{d}{h}\right) + 0.06\left(\frac{N}{h}\right) \leq 1$	
Yousefi et al. [58]	centred web holes: for unfastened flanges: $R_p = 0.98 - 0.65\left(\frac{d}{h}\right) + 0.07\left(\frac{N}{h}\right) \leq 1$	ITF
	for fastened flanges: $R_p = 0.99 - 0.04\left(\frac{d}{h}\right) + 0.03\left(\frac{N}{h}\right) \leq 1$	
	offset web holes: for unfastened flanges: $R_p = 0.94 - 0.62\left(\frac{d}{h}\right) + 0.21\left(\frac{x}{h}\right) \leq 1$	
	for fastened flanges: $R_p = 0.94 - 0.48\left(\frac{d}{h}\right) + 0.26\left(\frac{x}{h}\right) \leq 1$	
Uzzaman et al. [35]	centred web holes: $R_p = 1.02 - 0.39\left(\frac{d}{h}\right) + 0.02\left(\frac{N}{h}\right) + 0.04\left(\frac{r_q}{t}\right) + 0.49\left(\frac{q}{h}\right) \leq 1$	ITF, edge-stiffened holes
	offset web holes: $R_p = 1.01 - 0.16\left(\frac{d}{h}\right) + 0.06\left(\frac{x}{h}\right) + 0.04\left(\frac{r_q}{t}\right) + 0.31\left(\frac{q}{h}\right) \leq 1$	
Sivakumaran and Zielonka [60]	$R_p = \left[1 - 0.197\left(\frac{d}{h}\right)^2\right] \left[1 - 0.127\left(\frac{b}{n}\right)^2\right]$	IOF
Langan et al. [61]	$R_p = 0.964 - 0.272\left(\frac{d}{h}\right) + 0.0631\alpha \leq 1$ $\alpha \geq 4.31\left(\frac{d}{h}\right) + 0.571 \geq 0$	IOF
Lian et al. [55]	centred web holes: for unfastened flanges: $R_p = 0.98 - 0.26\left(\frac{d}{h}\right) + 0.06\left(\frac{N}{h}\right) \leq 1$	IOF
	for fastened flanges: $R_p = 0.95 - 0.06\left(\frac{d}{h}\right) + 0.01\left(\frac{N}{h}\right) \leq 1$	
	offset web holes: for unfastened flanges: $R_p = 0.99 - 0.26\left(\frac{d}{h}\right) + 0.11\left(\frac{x}{h}\right) \leq 1$	
	for fastened flanges: $R_p = 0.99 - 0.14\left(\frac{d}{h}\right) + 0.07\left(\frac{x}{h}\right) \leq 1$	
Langan et al. [61]	$R_p = 1.08 - 0.63\left(\frac{d}{h}\right) + 0.12\alpha \leq 1$ $\alpha \geq 5.25\left(\frac{d}{h}\right) - 0.67 \geq 0$	EOF

Table A3. Cont.

Reference	Equation	Note	
Lian et al. [53]	centred web holes: for unfastened flanges: $R_p = 0.96 - 0.34\left(\frac{d}{h}\right) + 0.09\left(\frac{N}{h}\right) \leq 1$	EOF	
	for fastened flanges: $R_p = 0.93 - 0.41\left(\frac{d}{h}\right) + 0.16\left(\frac{N}{h}\right) \leq 1$		
	offset web holes: for unfastened flanges: $R_p = 0.97 - 0.26\left(\frac{d}{h}\right) + 0.14\left(\frac{x}{h}\right) \leq 1$		
	for fastened flanges: $R_p = 0.97 - 0.14\left(\frac{d}{h}\right) + 0.07\left(\frac{x}{h}\right) \leq 1$		
	for unfastened flanges: $R_p = 0.90 - 0.60\left(\frac{d}{h}\right) + 0.12\left(\frac{N}{h}\right) \leq 1$		
	for fastened flanges: $R_p = 0.95 - 0.50\left(\frac{d}{h}\right) + 0.08\left(\frac{N}{h}\right) \leq 1$		
Uzzaman et al. [51]	for unfastened flanges: $R_p = 0.95 - 0.49\left(\frac{d}{h}\right) + 0.17\left(\frac{x}{h}\right) \leq 1$	ETF	
	for fastened flanges: $R_p = 0.96 - 0.36\left(\frac{d}{h}\right) + 0.14\left(\frac{x}{h}\right) \leq 1$		
	for unfastened flanges: $R_p = 0.92 - 0.35\left(\frac{d}{h}\right) + 0.12\left(\frac{N}{h}\right) + 0.21\left(\frac{r_q}{t}\right) + 0.22\left(\frac{q}{h}\right) \leq 1$		
Uzzaman et al. [34]	offset web holes: $R_p = 0.98 - 0.11\left(\frac{d}{h}\right) + 0.01\left(\frac{x}{h}\right) + 0.05\left(\frac{r_q}{t}\right) + 0.41\left(\frac{q}{h}\right) \leq 1$	ETF, edge-stiffened holes	

Table A4. Design equations in shear.

Reference	Equation	Note
Eiler et al. [66]	$V_{nl} = q_{s1} \cdot q_{s2} \cdot V_n$	
	$q_{s1} = \frac{1}{54} \cdot \frac{c_1}{t}, \text{ for } 5 \leq \frac{c_1}{t} \leq 54$	
	$q_{s1} = 1, \text{ for } \frac{c_1}{t} > 54$	
	$q_{s2} = 1.5 \cdot \frac{V_1}{V_2} - 0.5 \leq 1.3, \text{ for } \frac{c_1}{t} \leq 54$	
	$q_{s2} = 1, \text{ for } \frac{c_1}{t} > 54$	
	$c_1 = \frac{h}{2} - \frac{d}{2.83}, \text{ for circular holes}$ $c_1 = \frac{h}{2} - \frac{d}{2}, \text{ for square holes}$	
C.H. Pham [43]	circular holes: $k_v = k_0 \left[1 - 0.5\left(\frac{d}{L}\right) - 4.2\left(\frac{d}{L}\right)^2 \right], \text{ for } \frac{d}{L} \leq 0.2$	
	$k_v = k_0 \left[1.15 - 2.35\left(\frac{d}{L}\right) + 1.5\left(\frac{d}{L}\right)^2 \right], \text{ for } 0.2 < \frac{d}{L} \leq 0.6$	
	$k_v = k_0 \left[0.6 - 0.53\left(\frac{d}{L}\right) \right], \text{ for } \frac{d}{L} \geq 0.6$	
	square holes: $k_v = k_0 \left[1 - 0.8\left(\frac{d}{L}\right) - 4.5\left(\frac{d}{L}\right)^2 \right], \text{ for } \frac{d}{L} \leq 0.2$	
	$k_v = k_0 \left[1.15 - 2.95\left(\frac{d}{L}\right) + 2.2\left(\frac{d}{L}\right)^2 \right], \text{ for } 0.2 < \frac{d}{L} \leq 0.6$	
	$k_v = k_0 \left[0.4 - 0.33\left(\frac{d}{L}\right) \right], \text{ for } \frac{d}{L} \geq 0.6$ $k_0 = 5.34 + \frac{4}{\left(\frac{t}{h}\right)^2}$	

Table A4. Cont.

Reference	Equation	Note
Keerthan and Mahendran [67]	$V_{nl} = q_s \cdot V_v$	
	option 1:	
	$q_s = 1 - 0.6\left(\frac{d}{h}\right)$, for $0 < \frac{d}{h} \leq 0.3$	
	$q_s = 1.215 - 1.316\left(\frac{d}{h}\right)$, for $0.3 < \frac{d}{h} \leq 0.7$ $q_s = 0.732 - 0.625\left(\frac{d}{h}\right)$, for $0.7 < \frac{d}{h} \leq 0.85$	
option 2:		
	$q_s = 1 - 0.6\left(\frac{d}{h}\right)$, for $0 < \frac{d}{h} \leq 0.3$ $q_s = 1.224 - 1.346\left(\frac{d}{h}\right)$, for $0.3 < \frac{d}{h} \leq 0.85$	
S.H. Pham [44]	$V_{yh} = V_y$, for $0 < \frac{d}{h} \leq 0.1$ $V_{yh} = V_y - 2\left(\frac{d}{h} - 0.1\right)(V_y - V_{vrd,0.6})$, for $0.1 < \frac{d}{h} < 0.6$ $V_{yh} = V_{vrd}$, for $\frac{d}{h} \geq 0.6$ $V_{vrd} = \frac{4M_{pv}}{b}$	
D.K. Pham et al. [45]	$V_{yh} = 0.6A_w f_y = V_y$, for $0 < \frac{d}{h} \leq 0.1$ $V_{yh} = V_y - \left(\frac{1}{m-0.1}\right)\left(\frac{d}{h} - 0.1\right)(V_y - V_{vrd,m} \cdot v_i)$, for $0.1 < \frac{d}{h} < m$ $V_{yh} = V_{vrd} \cdot v_i$, for $\frac{d}{h} \geq m$ $m = 0.715 - 0.125\left(\frac{b}{d}\right) + 0.01\left(\frac{b}{d}\right)^2$, $v_i = 0.745 + 0.28\left(\frac{b}{d}\right) - 0.025\left(\frac{b}{d}\right)^2$	
C.H. Pham and Hancock [46]	$k_v = k_0 \left[1 - 0.8\left(\frac{d}{L}\right) - 4.5\left(\frac{d}{L}\right)^2\right]$, for $\frac{d}{L} \leq 0.2$ $k_v = k_0 \left[1.15 - 2.95\left(\frac{d}{L}\right) + 2.2\left(\frac{d}{L}\right)^2\right]$, for $0.2 < \frac{d}{L} \leq 0.6$ $k_v = k_0 \left[0.4 - 0.33\left(\frac{d}{L}\right)\right]$, for $\frac{d}{L} \geq 0.6$ $V_{yh} = 0.6(d_1 - d) \cdot t \cdot f_y$	

References

- Yu, W.; Davis, C.S. Buckling Behavior and Post-Buckling Strength of Perforated Stiffened Compression Elements. In Proceedings of the International Specialty Conference on Cold-Formed Steel Structures, Rolla, MI, USA, 19–20 August 1971.
- Moen, C.D.; Schafer, B.W. Experiments on Cold-Formed Steel Columns with Holes. *Thin-Walled Struct.* **2008**, *46*, 1164–1182. [\[CrossRef\]](#)
- Moen, C.D.; Schafer, B.W. Elastic Buckling of Cold-Formed Steel Columns and Beams with Holes. *Eng. Struct.* **2009**, *31*, 2812–2824. [\[CrossRef\]](#)
- Grey, C.N.; Moen, C.D. Elastic Buckling Simplified Methods for Cold-Formed Columns and Beams with Edge-Stiffened Holes. In Proceedings of the Annual Stability Conference Structural Stability Research Council Pittsburgh, Pittsburgh, PA, USA, 10–14 May 2011; pp. 92–103.
- Moen, C.D.; Schafer, B.W. Direct Strength Method for Design of Cold-Formed Steel Columns with Holes. *J. Struct. Eng.* **2011**, *137*, 559–570. [\[CrossRef\]](#)
- Kulatunga, M.P.; Macdonald, M. Investigation of Cold-Formed Steel Structural Members with Perforations of Different Arrangements Subjected to Compression Loading. *Thin-Walled Struct.* **2013**, *67*, 78–87. [\[CrossRef\]](#)
- Smith, F.H.; Moen, C.D. Finite Strip Elastic Buckling Solutions for Thin-Walled Metal Columns with Perforation Patterns. *Thin-Walled Struct.* **2014**, *79*, 187–201. [\[CrossRef\]](#)
- Kulatunga, M.P.; Macdonald, M.; Rhodes, J.; Harrison, D.K. Load Capacity of Cold-Formed Column Members of Lipped Channel Cross-Section with Perforations Subjected to Compression Loading—Part I: FE Simulation and Test Results. *Thin-Walled Struct.* **2014**, *80*, 1–12. [\[CrossRef\]](#)
- Wang, C.; Zhang, Z.; Zhao, D.; Bai, Y. Experimental and Numerical Study on Perforated Channel Columns with Complex Edge Stiffeners and Web Stiffeners. *Adv. Struct. Eng.* **2015**, *18*, 1303–1318. [\[CrossRef\]](#)
- Wang, C.; Bai, Y.; Liu, Q.; Zhao, D. Stability Behavior of Perforated Lipped Channel Columns. In Proceedings of the MATEC Web of Conferences, Hong Kong, China, 11–12 June 2016; Volume 67.
- Yao, Z.; Rasmussen, K.J.R. Perforated Cold-Formed Steel Members in Compression. I: Parametric Studies. *J. Struct. Eng.* **2016**, *143*, 04016226. [\[CrossRef\]](#)

12. Yao, Z.; Rasmussen, K.J.R. Perforated Cold-Formed Steel Members in Compression. II: Design. *J. Struct. Eng.* **2016**, *143*, 04016227. [[CrossRef](#)]
13. Chen, B.; Roy, K.; Uzzaman, A.; Raftery, G.M.; Nash, D.; Clifton, G.C.; Pouladi, P.; Lim, J.B.P. Effects of Edge-Stiffened Web Openings on the Behaviour of Cold-Formed Steel Channel Sections under Compression. *Thin-Walled Struct.* **2019**, *144*, 106307. [[CrossRef](#)]
14. Chen, B.; Roy, K.; Uzzaman, A.; Raftery, G.M.; Lim, J.B.P. Parametric Study and Simplified Design Equations for Cold-Formed Steel Channels with Edge-Stiffened Holes under Axial Compression. *J. Constr. Steel Res.* **2020**, *172*, 106161. [[CrossRef](#)]
15. Chen, B.; Roy, K.; Uzzaman, A.; Raftery, G.M.; Lim, J.B.P. Axial Strength of Back-to-Back Cold-Formed Steel Channels with Edge-Stiffened Holes, Un-Stiffened Holes and Plain Webs. *J. Constr. Steel Res.* **2020**, *174*, 106313. [[CrossRef](#)]
16. Xiang, Y.; Zhou, X.; Shi, Y.; Xu, L.; Xu, Y. Experimental Investigation and Finite Element Analysis of Cold-Formed Steel Channel Columns with Complex Edge Stiffeners. *Thin-Walled Struct.* **2020**, *152*, 106769. [[CrossRef](#)]
17. Ling, J.Y.; Kong, S.L.; De'nan, F. Numerical Study of Buckling Behaviour of Cold-Formed C-Channel Steel Purlin with Perforation. *Procedia Eng.* **2015**, *125*, 1135–1141. [[CrossRef](#)]
18. Wang, L.; Young, B. Design of Cold-Formed Steel Built-up Sections with Web Perforations Subjected to Bending. *Thin-Walled Struct.* **2017**, *120*, 458–469. [[CrossRef](#)]
19. Yuan, W.-b.; Yu, N.-t.; Li, L.-y. Distortional Buckling of Perforated Cold-Formed Steel Channel-Section Beams with Circular Holes in Web. *Int. J. Mech. Sci.* **2017**, *126*, 255–260. [[CrossRef](#)]
20. Yu, N.T.; Kim, B.; Yuan, W.-b.; Li, L.-y.; Yu, F. An Analytical Solution of Distortional Buckling Resistance of Cold-Formed Steel Channel-Section Beams with Web Openings. *Thin-Walled Struct.* **2019**, *135*, 446–452. [[CrossRef](#)]
21. Zhao, J.; Sun, K.; Yu, C.; Wang, J. Tests and Direct Strength Design on Cold-Formed Steel Channel Beams with Web Holes. *Eng. Struct.* **2019**, *184*, 434–446. [[CrossRef](#)]
22. Chen, B.; Roy, K.; Fang, Z.; Uzzaman, A.; Raftery, G.; Lim, J.B.P. Moment Capacity of Back-to-Back Cold-Formed Steel Channels with Edge-Stiffened Holes, Un-Stiffened Holes, and Plain Webs. *Eng. Struct.* **2021**, *235*, 112042. [[CrossRef](#)]
23. Shan, M.-Y.; LaBoube, R. *Behavior of Web Elements with Openings Subjected to Bending, Shear and the Combination of Bending and Shear*; Department of Civil Engineering, University of Missouri-Rolla: Rolla, MI, USA, 1994.
24. Shan, M.Y.; Batson, K.D.; LaBoube, R.A.; Yu, W.W. Local Buckling Flexural Strength of Webs with Openings. *Eng. Struct.* **1994**, *16*, 317–323. [[CrossRef](#)]
25. Shan, M.Y.; LaBoube, R.A.; Yu, W.W. Bending and Shear Behavior of Web Elements with Openings. *J. Struct. Eng.* **1996**, *122*, 854–859. [[CrossRef](#)]
26. Hancock, G.J. Design for Distortional Buckling of Flexural Members. *Thin-Walled Struct.* **1997**, *27*, 3–12. [[CrossRef](#)]
27. Moen, C.D.; Schafer, B.W. Extending Direct Strength Design to Cold-Formed Steel Beams with Holes. In Proceedings of the 20th International Specialty Conference on Cold-Formed Steel Structures, St. Louis, MO, USA, 3–4 November 2010.
28. Yu, C. Cold-Formed Steel Flexural Member with Edge Stiffened Holes: Behavior, Optimization, and Design. *J. Constr. Steel Res.* **2012**, *71*, 210–218. [[CrossRef](#)]
29. Moen, C.D.; Schudlich, A.; Von Der Heyden, A. Experiments on Cold-Formed Steel C-Section Joists with Unstiffened Web Holes. *J. Struct. Eng.* **2013**, *139*, 695–704. [[CrossRef](#)]
30. Wang, L.; Young, B. Beam Tests of Cold-Formed Steel Built-up Sections with Web Perforations. *J. Constr. Steel Res.* **2015**, *115*, 18–33. [[CrossRef](#)]
31. Dai, Y.; Roy, K.; Fang, Z.; Chen, B.; Raftery, G.M.; Lim, J.B.P. A Novel Machine Learning Model to Predict the Moment Capacity of Cold-Formed Steel Channel Beams with Edge-Stiffened and Un-Stiffened w.Pdf. *J. Build. Eng.* **2022**, *53*, 104592. [[CrossRef](#)]
32. Wang, C.; Guo, Q.; Zhang, Z.; Guo, Y. Experimental and Numerical Investigation of Perforated Cold-Formed Steel Built-up I-Section Columns with Web Stiffeners and Complex Edge Stiffeners. *Adv. Struct. Eng.* **2019**, *22*, 2205–2221. [[CrossRef](#)]
33. Uzzaman, A.; Lim, J.B.P.; Nash, D.; Young, B. Effects of Edge-Stiffened Circular Holes on the Web Crippling Strength of Cold-Formed Steel Channel Sections under One-Flange Loading Conditions. *Eng. Struct.* **2017**, *139*, 96–107. [[CrossRef](#)]
34. Uzzaman, A.; Lim, J.B.P.; Nash, D.; Roy, K. Cold-Formed Steel Channel Sections under End-Two-Flange Loading Condition: Design for Edge-Stiffened Holes, Unstiffened Holes and Plain Webs. *Thin-Walled Struct.* **2020**, *147*, 106532. [[CrossRef](#)]
35. Uzzaman, A.; Lim, J.B.P.; Nash, D.; Roy, K. Web Crippling Behaviour of Cold-Formed Steel Channel Sections with Edge-Stiffened and Unstiffened Circular Holes under Interior-Two-Flange Loading Condition. *Thin-Walled Struct.* **2020**, *154*, 106813. [[CrossRef](#)]
36. Chen, B.; Roy, K.; Fang, Z.; Uzzaman, A.; Chi, Y.; Lim, J.B.P. Web Crippling Capacity of Fastened Cold-Formed Steel Channels with Edge-Stiffened Web Holes, Un-Stiffened Web Holes and Plain Webs under Two-Flange Loading. *Thin-Walled Struct.* **2021**, *163*, 107666. [[CrossRef](#)]
37. Loov, R. Local Buckling Capacity of C-Shaped Cold-Formed Steel Sections with Punched Webs. *Can. J. Civ. Eng.* **1984**, *11*, 1–7. [[CrossRef](#)]
38. Pu, Y.; Godley, M.H.; Beale, R.G.; Lau, H.H. Prediction of Ultimate Capacity of Perforated Lipped Channels. *J. Struct. Eng.* **1999**, *125*, 510–514. [[CrossRef](#)]
39. Abdel-Rahman, N.; Sivakumaran, K.S. Effective Design Width for Perforated Cold-Formed Steel Compression Members. *Can. J. Civ. Eng.* **1998**, *25*, 319–330. [[CrossRef](#)]
40. Shanmugam, N.E.; Dhanalakshmi, M. Design for Openings in Cold-Formed Steel Channel Stub Columns. *Thin-Walled Struct.* **2001**, *39*, 961–981. [[CrossRef](#)]

41. Yao, Z.; Rasmussen, K.J.R. Inelastic Local Buckling Behaviour of Perforated Plates and Sections under Compression. *Thin-Walled Struct.* **2012**, *61*, 49–70. [[CrossRef](#)]
42. Yao, Z.; Rasmussen, K.J.R. *Design of Perforated Thin-Walled Steel Columns*; School of Civil Engineering, The University of Sydney: Sydney, Australia, 2014.
43. Pham, C.H. Shear Buckling of Plates and Thin-Walled Channel Sections with Holes. *J. Constr. Steel Res.* **2017**, *128*, 800–811. [[CrossRef](#)]
44. Pham, S.H. *Design of Cold-Formed Steel Beams with Holes and Transverse Stiffeners in Shear*; School of Civil Engineering, The University of Sydney: Sydney, Australia, 2018.
45. Pham, D.K.; Pham, C.H.; Pham, S.H.; Hancock, G.J. Experimental Investigation of High Strength Cold-Formed Channel Sections in Shear with Rectangular and Slotted Web Openings. *J. Constr. Steel Res.* **2020**, *165*, 105889. [[CrossRef](#)]
46. Pham, C.H.; Hancock, G.J. Shear Tests and Design of Cold-Formed Steel Channels with Central Square Holes. *Thin-Walled Struct.* **2020**, *149*, 106650. [[CrossRef](#)]
47. LaBoube, R.A.; Yu, W.W.; Deshmukh, S.U.; Uphoff, C.A. Crippling Capacity of Web Elements with Openings. *J. Struct. Eng.* **1999**, *125*, 137–141. [[CrossRef](#)]
48. Uzzaman, A.; Lim, J.B.P.; Nash, D.; Rhodes, J.; Young, B. Web Crippling Behaviour of Cold-Formed Steel Channel Sections with Offset Web Holes Subjected to Interior-Two-Flange Loading. *Thin-Walled Struct.* **2012**, *50*, 76–86. [[CrossRef](#)]
49. Uzzaman, A.; Lim, J.B.P.; Nash, D.; Rhodes, J.; Young, B. Cold-Formed Steel Sections with Web Openings Subjected to Web Crippling under Two-Flange Loading Conditions—Part I: Tests and Finite Element Analysis. *Thin-Walled Struct.* **2012**, *56*, 38–48. [[CrossRef](#)]
50. Uzzaman, A.; Lim, J.B.P.; Nash, D.; Rhodes, J.; Young, B. Cold-Formed Steel Sections with Web Openings Subjected to Web Crippling under Two-Flange Loading Conditions—Part II: Parametric Study and Proposed Design Equations. *Thin-Walled Struct.* **2012**, *56*, 79–87. [[CrossRef](#)]
51. Uzzaman, A.; Lim, J.B.P.; Nash, D.; Rhodes, J.; Young, B. Effect of Offset Web Holes on Web Crippling Strength of Cold-Formed Steel Channel Sections under End-Two-Flange Loading Condition. *Thin-Walled Struct.* **2013**, *65*, 34–48. [[CrossRef](#)]
52. Lian, Y.; Uzzaman, A.; Lim, J.B.P.; Abdelal, G.; Nash, D.; Young, B. Effect of Web Holes on Web Crippling Strength of Cold-Formed Steel Channel Sections under End-One-Flange Loading Condition—Part I: Tests and Finite Element Analysis. *Thin-Walled Struct.* **2016**, *107*, 443–452. [[CrossRef](#)]
53. Lian, Y.; Uzzaman, A.; Lim, J.B.P.; Abdelal, G.; Nash, D.; Young, B. Effect of Web Holes on Web Crippling Strength of Cold-Formed Steel Channel Sections under End-One-Flange Loading Condition—Part II: Parametric Study and Proposed Design Equations. *Thin-Walled Struct.* **2016**, *107*, 489–501. [[CrossRef](#)]
54. Lian, Y.; Uzzaman, A.; Lim, J.B.P.; Abdelal, G.; Nash, D.; Young, B. Web Crippling Behaviour of Cold-Formed Steel Channel Sections with Web Holes Subjected to Interior-One-Flange Loading Condition—Part I: Experimental and Numerical Investigation. *Thin-Walled Struct.* **2017**, *111*, 103–112. [[CrossRef](#)]
55. Lian, Y.; Uzzaman, A.; Lim, J.B.P.; Abdelal, G.; Nash, D.; Young, B. Web Crippling Behaviour of Cold-Formed Steel Channel Sections with Web Holes Subjected to Interior-One-Flange Loading Condition—Part II: Parametric Study and Proposed Design Equations. *Thin-Walled Struct.* **2017**, *114*, 92–106. [[CrossRef](#)]
56. Fang, Z.; Roy, K.; Liang, H.; Poologanathan, K.; Ghosh, K.; Mohamed, A.M.; Lim, J.B.P. Numerical Simulation and Design Recommendations for Web Crippling Strength of Cold-Formed Steel Channels with Web Holes under Interior-One-Flange Loading at Elevated Temperatures. *Buildings* **2021**, *11*, 666. [[CrossRef](#)]
57. Yousefi, A.M.; Lim, J.B.P.; Charles Clifton, G. Cold-Formed Ferritic Stainless Steel Unlipped Channels with Web Openings Subjected to Web Crippling under Interior-Two-Flange Loading Condition—Part I: Tests and Finite Element Model Validation. *Thin-Walled Struct.* **2017**, *116*, 333–341. [[CrossRef](#)]
58. Yousefi, A.M.; Lim, J.B.P.; Clifton, G.C. Cold-Formed Ferritic Stainless Steel Unlipped Channels with Web Openings Subjected to Web Crippling under Interior-Two-Flange Loading Condition—Part II: Parametric Study and Design Equations. *Thin-Walled Struct.* **2017**, *116*, 342–356. [[CrossRef](#)]
59. Davis, C.S.; Yu, W.W. *The Structural Behavior of Cold-Formed Steel Members with Perforated Elements*; Department of Civil Engineering, University of Missouri-Rolla: Rolla, MI, USA, 1972.
60. Sivakumaran, K.S.; Zielonka, K.M. Web Crippling Strength of Thin-Walled Steel Members with Web Opening. *Thin-Walled Struct.* **1989**, *8*, 295–319. [[CrossRef](#)]
61. Langan, E.J.; LaBoube, R.A.; Yu, W. *Structural Behavior of Perforated Web Elements of Cold-Formed Steel Flexural Members Subjected to Web Crippling and a Combination of Web Crippling and Bending*; Department of Civil Engineering, University of Missouri-Rolla: Rolla, MI, USA, 1994.
62. Deshmukh, S.U.; LaBoube, R.A.; Yu, W. *Behavior of Cold-Formed Steel Web Elements with Web Openings Subjected to Web Crippling and a Combination of Bending and Web Crippling for Interior-One-Flange Loading*; Department of Civil Engineering, University of Missouri-Rolla: Rolla, MI, USA, 1996.
63. Uphoff, C.A.; LaBoube, R.A.; Yu, W. *Structural Behavior of Circular Holes in Web Elements of Cold-Formed Steel Flexural Members Subjected to Web Crippling for End-One-Flange Loading*; Department of Civil Engineering, University of Missouri-Rolla: Rolla, MI, USA, 1996.

64. Fang, Z.; Roy, K.; Chi, Y.; Chen, B.; Lim, J.B.P. Finite Element Analysis and Proposed Design Rules for Cold-Formed Stainless Steel Channels with Web Holes under End-One-Flange Loading. *Structures* **2021**, *34*, 2876–2899. [[CrossRef](#)]
65. Fang, Z.; Roy, K.; Uzzaman, A.; Lim, J.B.P. Numerical Simulation and Proposed Design Rules of Cold-Formed Stainless Steel Channels with Web Holes under Interior-One-Flange Loading. *Eng. Struct.* **2022**, *252*, 113566. [[CrossRef](#)]
66. Eiler, M.; Laboube, R.; Yu, W. *Behavior of Web Elements with Openings Subjected to Linearly Varying Shear*; Department of Civil Engineering, University of Missouri-Rolla: Rolla, MI, USA, 1997.
67. Keerthan, P.; Mahendran, M. Experimental Studies of the Shear Behaviour and Strength of Lipped Channel Beams with Web Openings. *Thin-Walled Struct.* **2013**, *73*, 131–144. [[CrossRef](#)]
68. Keerthan, P.; Mahendran, M. Improved Shear Design Rules for Lipped Channel Beams with Web Openings. *J. Constr. Steel Res.* **2014**, *97*, 127–142. [[CrossRef](#)]
69. Pham, S.H.; Pham, C.H.; Rogers, C.A.; Hancock, G.J. New Proposals for the Direct Strength Method of Design of Cold-Formed Steel Beams with Holes in Shear. In Proceedings of the Wei-Wen Yu International Specialty Conference on Cold-Formed Steel Structures 2018, St. Louis, MO, USA, 7–8 November 2018; pp. 191–207.
70. Pham, S.H.; Pham, C.H.; Hancock, G.J. Experimental Study of Shear Strength of Cold-Formed Channels with an Aspect Ratio of 2.0. *J. Constr. Steel Res.* **2018**, *149*, 141–152. [[CrossRef](#)]
71. Pham, S.H.; Pham, C.H.; Hancock, G.J. Direct Strength Method of Design for Channel Sections in Shear with Square and Circular Web Holes. *J. Struct. Eng.* **2017**, *143*, 1–8. [[CrossRef](#)]
72. Pham, D.K.; Pham, C.H.; Hancock, G.J. Parametric Study for Shear Design of Cold-Formed Channels with Elongated Web Openings. *J. Constr. Steel Res.* **2020**, *172*, 106222. [[CrossRef](#)]
73. Acharya, S.R.; Sivakumaran, K.S.; Young, B. Reinforcement Schemes for Cold-Formed Steel Joists with a Large Web Opening in Shear Zone—An Experimental Investigation. *Thin-Walled Struct.* **2013**, *72*, 28–36. [[CrossRef](#)]
74. Madugula, M.K.S.; Ray, S.K. Ultimate Strength of Eccentrically Loaded Cold-Formed Angles. *Can. J. Civ. Eng.* **1984**, *11*, 225–233. [[CrossRef](#)]
75. Wang, C.; Zhang, Z.; Zhao, D.; Liu, Q. Compression Tests and Numerical Analysis of Web-Stiffened Channels with Complex Edge Stiffeners. *J. Constr. Steel Res.* **2016**, *116*, 29–39. [[CrossRef](#)]
76. Ma, J.-L.; Chan, T.-M.; Young, B. Investigation on Cold-Formed High Strength Steel Circular Hollow Sections under Combined Compression and Bending. In Proceedings of the Eurosteel 2017, Copenhagen, Denmark, 13–15 September 2017; Volume 1, pp. 3622–3630.
77. Merkl, C.; Toffolon, A.; Taras, A. Experimental and Numerical Study of the Behaviour of Eccentrically Loaded Cold-Formed Channel Sections—Determination of an Optimal Load Eccentricity. In Proceedings of the Eurosteel 2017, Copenhagen, Denmark, 13–15 September 2017; Volume 1, pp. 1553–1562.
78. Sadovský, Z.; Kriváček, J. Influence of Boundary Conditions and Load Eccentricity on Strength of Cold-Formed Lipped Channel Columns. *Thin-Walled Struct.* **2018**, *131*, 556–565. [[CrossRef](#)]
79. Ghandi, E.; Niari, S.E. Flexural-Torsional Buckling of Cold-Formed Steel Columns with Arbitrary Cross-Section under Eccentric Axial Load. *Structures* **2020**, *28*, 2122–2134. [[CrossRef](#)]
80. Meza, F.J.; Becque, J.; Hajirasouliha, I. Experimental Study of Cold-Formed Steel Built-up Columns. *Thin-Walled Struct.* **2020**, *149*, 106291. [[CrossRef](#)]
81. Chen, M.T.; Young, B. Beam-Column Tests of Cold-Formed Steel Elliptical Hollow Sections. *Eng. Struct.* **2020**, *210*, 109911. [[CrossRef](#)]
82. Peiris, M.; Mahendran, M. Behaviour of Cold-Formed Steel Lipped Channel Sections Subject to Eccentric Axial Compression. *J. Constr. Steel Res.* **2021**, *184*, 106808. [[CrossRef](#)]
83. Zhang, J.-F.; Wang, B.; Wang, S.; Deng, E.-F.; Zhang, P.; Pang, S.-Y.; Wen, M.-G.; Ye, L.; Guo, X.-S.; Gao, J. Eccentric Compressive Distortional Buckling and Design of Non-Symmetric Cold-Formed Angular Column with Complex Edges. *Thin-Walled Struct.* **2021**, *165*, 107981. [[CrossRef](#)]
84. Li, Q.-Y.; Young, B. Tests of Cold-Formed Steel Built-up Open Section Members under Eccentric Compressive Load. *J. Constr. Steel Res.* **2021**, *184*, 106775. [[CrossRef](#)]
85. Bonada, J.; Pastor, M.M.; Roure, F.; Casafont, M. Distortional Influence of Pallet Rack Uprights Subject to Combined Compression and Bending. *Structures* **2016**, *8*, 275–285. [[CrossRef](#)]
86. Bertocci, L.; Comparini, D.; Lavacchini, G.; Orlando, M.; Salvatori, L.; Spinelli, P. Experimental, Numerical, and Regulatory P-Mx-My Domains for Cold-Formed Perforated Steel Uprights of Pallet-Racks. *Thin-Walled Struct.* **2017**, *119*, 151–165. [[CrossRef](#)]
87. Pastor, M.M.; Bonada, J.; Roure, F.; Casafont, M.; Somalo, M.R. Rack Uprights under Combined Compression and Bi-Axial Bending: Experimental Testing, Numerical Analysis and European Standard Approach. In Proceedings of the Eurosteel 2017, Copenhagen, Denmark, 13–15 September 2017; Volume 1, pp. 1609–1616.
88. Orlando, M.; Lavacchini, G.; Ortolani, B.; Spinelli, P. Experimental Capacity of Perforated Cold-Formed Steel Open Sections under Compression and Bending. *Steel Compos. Struct.* **2017**, *24*, 201–211. [[CrossRef](#)]
89. *AISI S100-2016*; North American Specification for the Design of Cold-Formed Steel Structural Members. American Iron and Steel Institute: Washington, DC, USA, 2016.
90. *EN 1993-1-3*; Eurocode 3: Design of Steel Structures—Part 1–3: General Rules—Supplementary Rules for Cold-Formed Members and Sheeting. European Committee for Standardization: Brussels, Belgium, 2006.

91. AS/NZS 4600: 2018; Cold-Formed Steel Structures. AustralianNew Zealand Standard: Sydney, Australia; Wellington, New Zealand, 2018.
92. GB50018-2002; Technical Code of Cold-Formed Thin-Wall Steel Structures. General Administration of Quality Supervision Inspection and Quarantine: Beijing, China, 2002.
93. American Iron and Steel Institute. *Specification for the Design of Light Gage Steel Structural Members*; American Iron and Steel Institute: New York, NY, USA, 1946.
94. EN 15512; Steel Static Storage Systems—Adjustable Pallet Racking Systems—Principles for Structural Design. European Committee for Standardization: Brussels, Belgium, 2009.
95. Dubina, D.; Ungureanu, V.; Landolfo, R. *Design of Cold-Formed Steel Structures*; European Convention for Constructional Steelwork: Brussels, Belgium, 2012; ISBN 978-92-9147-107-2.
96. Ádány, S.; Silvestre, N.; Schafer, B.W.; Camotim, D. GBT and CFSM: Two Modal Approaches to the Buckling Analysis of Unbranched Thin-Walled Members. *Adv. Steel Constr.* **2009**, *5*, 195–223.
97. Casafont, M.; Pastor, M.M.; Roure, F.; Bonada, J.; Peköz, T. Design of Steel Storage Rack Columns via the Direct Strength Method. *J. Struct. Eng.* **2013**, *139*, 669–679. [[CrossRef](#)]
98. Li, Z.; Schafer, B.W. Constrained Finite Strip Method for Thin-Walled Members with General End Boundary Conditions. *J. Eng. Mech.* **2013**, *139*, 1566–1576. [[CrossRef](#)]
99. Li, Z.; Schafer, B.W. Buckling Analysis of Cold-Formed Steel Members with General Boundary Conditions Using CUFSM: Conventional and Constrained Finite Strip Methods. In Proceedings of the 20th International Specialty Conference on Cold-Formed Steel Structures, St. Louis, MO, USA, 3–4 November 2010.
100. Moen, C.D. Direct Strength Design of Cold-Formed Steel Members with Perforations. Ph.D. Dissertation, Johns Hopkins University, Baltimore, MD, USA, 2008.
101. *Abaqus/CAE User's Guide*, Ver. 6.14, Dassault Systèmes Simulia Corp.: Providence, RI, USA, 2014.
102. Silvestre, N.; Camotim, D. First-Order Generalised Beam Theory for Arbitrary Orthotropic Materials. *Thin-Walled Struct.* **2002**, *40*, 755–789. [[CrossRef](#)]
103. Silvestre, N.; Camotim, D. Second-Order Generalised Beam Theory for Arbitrary Orthotropic Materials. *Thin-Walled Struct.* **2002**, *40*, 791–820. [[CrossRef](#)]
104. Abambres, M.; Camotim, D.; Silvestre, N. Modal Decomposition of Thin-Walled Member Collapse Mechanisms. *Thin-Walled Struct.* **2014**, *74*, 269–291. [[CrossRef](#)]
105. Bebiano, R.; Basaglia, C.; Camotim, D.; Gonçalves, R. GBT Buckling Analysis of Generally Loaded Thin-Walled Members with Arbitrary Flat-Walled Cross-Sections. *Thin-Walled Struct.* **2018**, *123*, 11–24. [[CrossRef](#)]
106. Bebiano, R.; Camotim, D.; Gonçalves, R. GBTUL 2.0—A Second-Generation Code for the GBT-Based Buckling and Vibration Analysis of Thin-Walled Members. *Thin-Walled Struct.* **2018**, *124*, 235–257. [[CrossRef](#)]
107. S136-1974; Cold Formed Steel Structural Members. Canadian Standards Association: Rexdale, ON, Canada, 1974.
108. Sivakumaran, K.S. Load Capacity of Uniformly Compressed Cold-Formed Steel Section with Punched Web. *Can. J. Civ. Eng.* **1987**, *14*, 550–558. [[CrossRef](#)]
109. Sivakumaran, K.S. Some Studies on Cold-Formed Steel Sections with Web Openings. In Proceedings of the Ninth International Specialty Conference on Cold-Formed Steel Structures, St. Louis, MO, USA, 8–9 November 1988.
110. AISI S100-1986; Specification for the Design of Cold-Formed Steel Structural Members Design. American Iron and Steel Institute: Washington, DC, USA, 1986.
111. Abdel-Rahman, N. *Cold-Formed Steel Compression Members with Perforations*; McMaster University: Hamilton, ON, Canada, 1997.
112. Yao, Z.; Rasmussen, K.J.R. Material and Geometric Nonlinear Isoparametric Spline Finite Strip Analysis of Perforated Thin-Walled Steel Structures—Analytical Developments. *Thin-Walled Struct.* **2011**, *49*, 1374–1391. [[CrossRef](#)]
113. Yao, Z.; Rasmussen, K.J.R. Material and Geometric Nonlinear Isoparametric Spline Finite Strip Analysis of Perforated Thin-Walled Steel Structures—Numerical Investigations. *Thin-Walled Struct.* **2011**, *49*, 1359–1373. [[CrossRef](#)]
114. AISI S100-2012; North American Specification for the Design of Cold-Formed Steel Structural Members. American Iron and Steel Institute: Washington, DC, USA, 2012.
115. BS 5950-5:1998; Structural Use of Steelwork in Building—Part 5. Code of Practice for Design of Cold Formed Thin Gauge Sections. British Standards Institution: London, UK, 1998; ISBN 0580282481.
116. Moen, C.D.; Schafer, B.W. *Direct Strength Design of Cold-Formed Steel Members with Perforations*; American Iron and Steel Institute: Washington, DC, USA, 2009.
117. AISI S100-2007; North American Specification for the Design of Cold-Formed Steel Structural Members. American Iron and Steel Institute: Washington, DC, USA, 2007.
118. Sivakumaran, K.S.; Ng, M.Y.; Fox, S.R. Flexural Strength of Cold-Formed Steel Joists with Reinforced Web Openings. *Can. J. Civ. Eng.* **2006**, *33*, 1195–1208. [[CrossRef](#)]
119. AISI S100-1968; Specification for the Design of Cold-Formed Steel Structural Members. American Iron and Steel Institute: Charlotte, NC, USA, 1968.
120. CAN3-S136-M84; Cold Formed Steel Structural Members. Canadian Standards Association: Rexdale, ON, Canada, 1984.
121. Lau, S.C.W.; Hancock, G.J. Buckling of Thin Flat-Walled Structures by a Spline Finite Strip Method. *Thin-Walled Struct.* **1986**, *4*, 269–294. [[CrossRef](#)]

122. AS/NZS4673 AS/NZS 4600:2005; Cold-Formed Steel Structures. Standards Australia/Standards New Zealand: Sydney, Australia, 2005.
123. LaBoube, R.A.; Yu, W.W.; Langan, J.E.; Shan, M.Y. Cold-Formed Steel Webs with Openings: Summary Report. *Thin-Walled Struct.* **1997**, *27*, 79–84. [[CrossRef](#)]
124. Chung, K.F.; Liu, T.C.H.; Ko, A.C.H. Investigation on Vierendeel Mechanism in Steel Beams with Circular Web Openings. *J. Constr. Steel Res.* **2001**, *57*, 467–490. [[CrossRef](#)]
125. ANSI/AISC 360-16; Specification for Structural Steel Buildings. American Institute of Steel Construction: Chicago, IL, USA, 2016.
126. American Iron and Steel Institute. *Load and Resistance Factor Design Specification for Cold-Formed Steel Structural Members*; American Iron and Steel Institute: Washington, DC, USA, 1991.